NATIONAL ADVISORY COMMITTEE FOR AERONAUTICS

WARTIME REPORT

ORIGINALLY ISSUED

September 1943 as
Advance [redacted] Report No. 3I30

CALCULATED AND MEASURED TURNING PERFORMANCE OF A NAVY F2A-3 AIRPLANE AS AFFECTED BY THE USE OF FLAPS

By Lawrence A. Clousing, Burnett L. Gadeberg,
and William M. Kauffman

Ames Aeronautical Laboratory
Moffett Field, Calif.

NACA

WASHINGTON

NATIONAL ADVISORY COMMITTEE FOR AERONAUTICS

ADVANCE [redacted] REPORT

CALCULATED AND MEASURED TURNING PERFORMANCE OF A NAVY F2A-3 AIRPLANE AS AFFECTED BY THE USE OF FLAPS

By Lawrence A. Clousing, Burnett L. Gadeberg, and William M. Kauffman

SUMMARY

Results of flight tests to determine the turning performance of a Navy F2A-3 airplane over a speed range of approximately 90 to 160 miles per hour for three flap deflections at two altitudes are presented. In general, for horizontal turns, the use of the standard airplane partial-span split flaps does not appear desirable for this airplane. For turns involving a loss of altitude, the turning radius is decreased by the use of the flaps.

The results of the flight tests have been correlated with an analytical study of turning performance in which the effect of thrust on maximum lift coefficient was considered. It was found that the turning performance of an airplane can be calculated with satisfactory accuracy by the method described.

INTRODUCTION

In order to arrive at a descriptive criterion of turning performance, several performance characteristics must be considered. The radius of curvature of the flight path described by the airplane, the time to turn through a given azimuth angle, and the loss of altitude in a given turn may be considered to be of paramount importance, since these are measures of the tightness of the turn, the rate of turn, and the ability of a combat plane to maintain or gain an altitude advantage over the opponent.

In previous methods of calculating the turning performance of airplanes, the effect of thrust upon the maximum lift coefficient has been neglected, and measurements

made in the present investigation consequently show a poor correlation with such calculations. In addition, the information available concerning the effect of flap deflection upon the turning performance and the effect of thrust upon the maximum lift coefficient has been inadequate for application to an actual problem. Consequently, when the Bureau of Aeronautics, Navy Department, requested that flight tests be carried out to determine the turning performance of a Navy F2A-3 airplane (No. 01516), in addition to the tests for this specific purpose, tests to determine the polar curves of the airplane for various flap deflections and the effect of thrust upon the maximum lift coefficient were made. The purpose of these latter tests was to establish data necessary to calculate turning performance. The tests necessary to determine turning performance itself were thus perhaps somewhat reduced in number, although they were carried out for two altitudes and three flap deflections.

APPARATUS

Description of the Navy F2A-3 airplane as flown.- The Navy F2A-3 airplane tested was a single-place, single-engine, midwing, pursuit-type, cantilever monoplane with retractable landing gear and partial-span split flaps. Figure 1 is a three-view drawing, and figures 2 and 3 show the airplane, with flaps down, as instrumented for the flight tests.

General specifications are as follows:

Airplane	Navy F2A-3, No. 01516
Engine	Wright 9 cylinder, R-1820-40. 1200 bhp at 2500 rpm and 45.5 inches of mercury manifold pressure for take-off, 1000 bhp at 2300 rpm and 37.3 inches of mercury manifold pressure at 6800 feet with blower in low-gear ratio. 900 bhp at 2300 rpm and 40.3 inches of mercury

	manifold pressure at 15,100 feet with blower in high-gear ratio.
Gear ratio	3:2
Propeller	Curtiss electric, constant speed.
Diameter	10 feet, 3 inches
Number of blades	3
Fuel capacity	160 gallons
Weight and balance, normal fighter:	
Gross weight	6515 pounds
Center of gravity aft of the leading edge	26.15 percent M.A.C.
Range of center of gravity	21.5 to 26.8 percent M.A.C.
Wing:	
Span	35 feet
Area (including 30.8 sq ft blanketed by the fuselage)	208.9 square feet
Airfoil	NACA 23000 series tapered by straight lines in plan form and thickness from root to tip. The root and tip thickness are 18-percent and 9-percent chord, respectively.
Incidence	0°

Mean aerodynamic chord . . . 74.88 inches

Flaps:

Length (each) . . . . . 8.47 feet

Area (each) . . . . . 8.22 square feet

Chord (max.) . . . . . 1.06 feet

INSTRUMENT INSTALLATION

NACA instruments were used to record photographically as a function of time the following variables: airspeed; normal, longitudinal, and lateral accelerations; pressure altitude; change of altitude; longitudinal inclination; rolling, yawing, and pitching velocities; manifold pressure; engine revolutions per minute; engine torque; and approximate angle of attack. Changes in azimuth during turns were determined by photographing the reading of a standard type directional gyroscope by means of a motion-picture camera which was synchronized with the other records. The free-air temperature was read from a standard-type airplane indicating thermometer.

The airspeed recorder was connected to a freely swiveling pitot-static head, which was vaned to align itself with the relative wind, and was located on a boom extending about a chord length ahead of the left wing tip (figs. 2 and 3). The position error of the airspeed head was found from flight tests to be negligible. The rates of air flow through the static and total-pressure tubes were so balanced that flight involving a change in air density would not cause an error in recorded airspeed. To minimize the effects of lag, the recorder itself was mounted at the base of the boom.

The directional gyroscope was mounted in an internally lighted box. A calibration was made of the error in azimuth reading created by operating the instrument at various angles of bank and pitch. Inasmuch as the directional gyroscope would not function properly when it was banked more than 55°, the instrument was mounted with an initial bank of 45° to the right. All turns were then made to the left. Thus, by uncaging the gyroscope in a left turn,

just prior to the time of taking records, it was possible to obtain large angles of left bank without malfunctioning of the gyroscope.

The approximate angle of attack was measured directly by a vane pivoted to align itself, in pitch, with the relative wind. The vane was mounted on a boom near the right wing tip and approximately one chord length ahead of the leading edge. Although, due to the upwash, this instrument did not give a true value of the angle of attack, the records were helpful in determining the proximity to the stall during the turning maneuvers. The angle of attack was determined more precisely in steady straight flight from data on change of altitude, true airspeed, and longitudinal inclination of the airplane.

Density altitude was determined from the measurements of pressure altitude and free-air temperature. The general term "altitude," as used hereafter in the text, denotes altitude in the standard atmosphere as determined by density.

The horsepower delivered by the engine was determined by the use of a Wright engine torquemeter and the revolutions per minute recorder.

SYMBOLS AND COEFFICIENTS

a	acceleration, feet per second per second
C_D	drag coefficient
C_{D_o}	effective profile-drag coefficient
C_L	lift coefficient
d	propeller diameter, feet
D	drag of airplane, pounds
F	force, pounds
g	acceleration of gravity, feet per second per second (32.2)

ΔH	change of absolute altitude in 360° turn, feet
K	$(\Delta C_L q S)/T_e$
L	lift of airplane, pounds
l_s	effective span loading, pounds per square foot
m	mass, slugs
q	dynamic pressure, pounds per square foot $(1/2\ \rho V^2)$
q_c	total pressure − static pressure, assumed to be equal to q in this report
R	radius of curvature of flight path, feet
r	radius of helix cylinder, feet
S	wing area, square feet
T_c	$\frac{T_e}{\rho V^2 d^2}$
T_c'	$\frac{T_e}{qS}$
T_e	effective propeller thrust, pounds
t	time to turn 360°, seconds
V	true airspeed, feet per second
V_i	correct indicated airspeed, miles per hour (defined by $V_i = 19.8\ \sqrt{q_c}$)
W	gross weight of airplane, pounds
$\frac{dC_D}{dC_L^2}$	$\frac{C_D - C_{D_o}}{C_L^2}$
γ	$\left(\frac{T_e - D_l}{W}\right)\ \frac{1}{l_s}$

$\Delta\gamma$ $\left(\frac{D_t - D_l}{W}\right) \frac{1}{l_s}$

θ inclination of flight path to horizontal, degrees

θ_o angle of climb in straight flight, degrees

σ ratio of air density at altitude to standard air density at sea level

φ angle of bank, degrees

ω angular velocity, radians per second

Subscripts:

h horizontal

L longitudinal

l straight flight

n normal

t turning flight

THEORETICAL CONSIDERATION OF THE CALCULATION AND MEASUREMENT OF TURNING PERFORMANCE

Throughout this report, the term "radius of curvature" is used in preference to the term "radius of turn," since some ambiquity may arise in considering spiral flight as to whether the term "radius of turn" refers to the radius of curvature of the flight path or the radius of the cylinder about which the spiral path is made. The relation between the radius of curvature of the flight path and that of the helix cylinder may be shown to be

$$r = R \cos^2\theta$$

The formula for computing the radius of curvature of the flight path of an airplane in steady turning flight may be developed as follows:

From Newton's second law of motion,

$$F = m a_h \tag{1}$$

Figure 4(a) shows that the force producing the horizontal, or radial, acceleration along the Y axis is

$$F = L \sin \varphi \tag{2}$$

The axes shown in figure 4(a) and 4(b) are mutually perpendicular. The Z axis is vertical, and the X axis lies in the vertical plane of the flight path of the airplane. The flight path is inclined to the X axis at an angle θ.

The equation for computing acceleration from speed and radius of curvature is known to be

$$a_h = \frac{V^2}{R} \tag{3}$$

where

$$V^2 = \frac{(1.47\ V_i)^2}{\sigma} \tag{4}$$

Figure 4(a) also shows that

$$F_y = L \cos \varphi$$

and

$$F_y = W \cos \theta$$

hence

$$L \cos \varphi = W \cos \theta \tag{5}$$

Substituting for F and a_h the values as derived from equations (2), (3), (4), and (5), and placing m equal to W/g and L equal to $C_L qS$ gives

$$R = \frac{(1.47\ V_i)^2}{\sigma g\left[\left(\frac{C_L qS}{W}\right)^2 - \cos^2\theta\right]^{1/2}} \qquad (6)$$

To use equation (6) to predict the radius of curvature at various speeds, certain information about the airplane must be available. This includes such items as weight, altitude, horsepower, revolutions per minute, and the lift-drag characteristics of the airplane, or at least sufficient of its geometry to estimate them.

In considering the application of equation (6) to the calculation of the minimum radius of curvature, it is apparent that the minimum radius of curvature at a given speed will be obtained at the maximum lift coefficient. The maximum lift coefficient attainable is dependent upon the thrust which is being delivered, and thus the variation of $C_{L_{max}}$ with thrust coefficient must be available. Knowing the variation of thrust with airspeed for the specified conditions, the variation of the maximum lift coefficient with airspeed for these conditions can be computed.

The angle θ is equal to $\sin^{-1}\left(\frac{T_e - D_t}{W}\right)$. Thus it is necessary to know C_{D_t} for the specified conditions and value of $C_{L_{max}}$.

While the above indicates the method for calculation of the radius of curvature in turns of minimum radius at various speeds, formula (6) can be used to predict the radius of curvature using any value of C_L less than $C_{L_{max}}$ for the speed desired. Since $\frac{C_L qS}{W/g} \approx a_n$, this amounts to predicting turns at various normal accelerations. To determine θ and airplane polar for the specified flap condition is required.

The time to turn through 360° can be found by considering the space and velocity components in the horizontal plane.

Thus

$$t = \frac{\text{distance}}{\text{velocity}} = \frac{2 \pi r}{V \cos \theta}$$

and using

$$r = R \cos^2 \theta$$

and equation (4)

$$t = \frac{2 \pi \sigma^{1/2} R \cos \theta}{1.47 V_i} \qquad (7)$$

The loss of altitude in a 360° turn is equal to the vertical component of velocity multiplied by the time to turn through 360°, or

$$\Delta H = 2 \pi R \sin \theta \cos \theta \qquad (8)$$

Horizontal turns for the specified conditions at various speeds may be considered as a special case where the flight path angle θ is zero.

Then

$$\frac{T_e - D_t}{W} = \sin \theta = 0$$

and

$$T = D_t = C_{D_t} qS \qquad (9)$$

Knowing the thrust for the desired speed, C_{D_t} can be computed from equation (9). The corresponding value of C_L is taken from the polar curve and substituted in equation (6) and the radius of curvature is determined.

For deriving radius of curvature from observed data, formulas were developed in which terms readily deduced from the observations were involved. In figure 4(b), the airplane normal and longitudinal accelerations, a_n and a_L, respectively, lie in a plane through the flight path

and inclined at an angle of bank φ to the XZ plane. The vector a_R is the vector sum of a_n and a_L and, for steady conditions, must lie in the ZY plane. For steady flight, a_h must lie along the Y axis and is equal to the vector sum of a_R and the gravitational acceleration g.

Therefore

$$a_h = \sqrt{a_n^2 + a_L^2 - g^2} \tag{10}$$

Rewriting the general equation (3)

$$R = \frac{V^2}{a_h} = \frac{(1.47\ V_i)^2}{\sigma\ a_h} \tag{11}$$

Since

$$V \cos \theta = r\ \omega$$

and

$$r = R \cos^2 \theta$$

$$R = \frac{V}{\omega \cos \theta} = \frac{1.47\ V_i}{\sigma^{1/2} \omega \cos \theta} \tag{12}$$

The value ω was determined directly from the photographically recorded indications of the directional gyroscope, or from the vector sum of the readings of the three turn meters which recorded the angular velocities about the airplane axes. The flight-path angle θ was determined with the aid of records of change of altitude.

TESTS

Airplane polars.- Airplane polars for the flaps-up, 22° down, and 56° down (full-down) conditions, with the landing gear up and the hood closed, were determined from a series of straight flights at altitudes between 4000 and 12,000 feet. These conditions of flaps, gear, and hood

corresponded to those used during the turn tests. Various powers from practically zero (throttle full back) to maximum rated were used during these tests.

The weight of the airplane for each run was determined from the known take-off weight, fuel consumption, and time of flight. The brake horsepower output was found from recorded torquemeter and revolutions per minute indicator readings. The effective thrust was calculated from brake horsepower, revolutions per minute, indicated airspeed, free-air temperature, and pressure-altitude readings, assuming an efficiency curve similar to that of a three-blade 5869-9 propeller. Power coefficient and efficiency curves for this propeller are given in reference 1. The flight-path angle θ was computed by use of the readings of airspeed and altitude.

Then

$$C_{L_l} = \frac{W \cos \theta}{qS} \tag{13}$$

and

$$C_{D_l} = \frac{T_e + W \sin \theta}{qS} \tag{14}$$

Due to the unsteady conditions existing during the stalls, it was not possible to determine the drag coefficients at $C_{L_{max}}$. However, numerous steady runs were made at speeds just above the stalling speed for the various flap and power conditions, and the results were extrapolated to $C_{L_{max}}$.

Effect of thrust on $C_{L_{max}}$.- The effect of thrust on $C_{L_{max}}$ was determined from the results of flight tests which consisted of a series of stalls with various power conditions from power-off to full-rated power and with various flap deflections. The flight tests were conducted at altitudes between 4000 and 12,000 feet. During the power-off runs, the propeller was placed in manual high pitch and hence delivered practically no effective thrust. In all of the stalls the airplane was pulled slowly from straight flight into a definitely stalled condition.

No corrections were made for change in $C_{L_{max}}$ due to the rate of change of angle of attack.

Turns.- Two types of turns were made, and in both the airplane was properly banked to give no acceleration along the airplane lateral axis. In the first type (turns at nearly $C_{L_{max}}$) maximum rated power was applied, and the airplane was pulled into the turn and held at a predetermined constant indicated airspeed. Each turn was tightened until stall warning in the form of buffeting was obtained. Airspeed was held constant by allowing the altitude to change. The airplane was then held as steady as possible at these conditions while the records were made.

In the second type (horizontal turns) each turn was started from straight level flight at the predetermined indicated airspeed. The turn was tightened and simultaneously power was applied to maintain constant speed and altitude, until maximum rated power was developed. Again, records were made while these conditions were held as steady as possible.

Both types of turns were made with flap settings of 0°, 22°, and 56° within a range of from 90° to 160-miles per hour indicated airspeeds, and at altitudes of about 13,000 and 27,000 feet. The test conditions of weight, altitude, and brake horsepower were held within the following limits:

Turns at nominal altitude of 13,000 feet:

Gross weight . . . . . 6,000 to 6,600 pounds

Altitude . . . . . 12,150 to 14,050 feet

(σ 0.690 to 0.649)

Brake horsepower . . . 740 to 860

Turns at nominal altitude of 27,000 feet:

Gross weight . . . . 5,900 to 6,550 pounds

Altitude . . . . . 24,750 to 27,950 feet

(σ 0.450 to 0.403)

Brake horsepower . . . 500 to 660

Though there were slight changes of equipment weight between the various test flights, the changes of airplane gross weight were due chiefly to fuel consumption during the flights. The variations of altitude resulted mainly from the difficulty of obtaining the desired altitude as the average for the recorded steady portions of the turns. The wide ranges of brake horsepower arose principally from mechanical difficulties experienced with the power plant. Three different engines were used during the turn-flight tests, and these engines were found to have different operating characteristics. Thus, when similar manifold pressures and engine speeds were employed, different brake horsepower outputs were obtained from each of the three engines. The brake horsepower of the third engine could only be approximated, as the recording torquemeter was not installed on this engine.

Due to occasional creeping, some difficulty was experienced by the pilots in maintaining the flap positions. Any runs in which the pilot indicated that this had occurred were dicarded.

Flight time.- The polar curves were obtained from 400 runs which required 20 hours of flying time. A total of 70 stalls was performed to obtain the $C_{L_{max}}$ data. Records were taken in a total of 262 turns which required 50 hours flying time.

RESULTS AND DISCUSSION

Airplane polars.- Plots of the polar curves of the airplane in the form of curves of C_L against C_D are shown in figure 5 for the three flap conditions tested. The equations for the parabolic curves plotted in figure 5 are also shown in the figure. These curves were derived from flight-test data by plotting C_L^2 against C_D for each flap condition and drawing a straight line through the points. The points plotted in the form of C_L^2 against C_D showed some scatter, especially in the high C_L^2 region. In this region, however, it was difficult to determine C_D.

accurately from flight measurements because of unsteadiness of the airplane, and the straight line relationship chosen thus seemed to be reasonable and was convenient to use. The scatter of the points did not seem to bear any relationship to the variation in thrust during the test runs, which would appear to indicate that the method used to determine propeller efficiency and thrust was acceptable for this airplane and propeller combination. The curves of figure 5 appeared to be representative of the mean relation of C_L to C_D even when, due to the action of the propeller, C_L became greater than the maximum for zero thrust.

Although the polar curves of the airplane may be different at various altitudes, due to the effects of different values of Reynolds and Mach numbers, such differences have been assumed to be negligible in the present investigation.

Effect of thrust on $C_{L_{max}}$.- The curves pertaining to the effects of thrust on $C_{L_{max}}$ are presented in figures 6 to 15. These curves were derived from flight-test data as follows. The approximate time of stalling was determined by inspection of the records for each of the stall runs, and computations of $C_{L_{max}}$ were then made. The power delivered to the propeller at the time of the stall was determined from the revolutions per minute and torquemeter indications, and the effective thrust was computed by the method previously explained for airplane polars. A thrust coefficient T_c' was then determined by the relation

$$T_c' = \text{a constant} \times T_c = \frac{2d^2}{S}\left(\frac{T_e}{\rho V^2 d^2}\right) = \frac{T_e}{qS}$$

The variations of $C_{L_{max}}$ with T_c' for various flap deflections are shown in figures 6 to 10. By plotting $C_{L_{max}}$ as a function of T_c' instead of T_c, the slope K is numerically equal to the ratio of the increase in lift, due to the propeller, to the effective thrust and is also the value of K used in reference 2.

Additional information is given in figures 11 and 12. The variation of K with flap deflection shows that at a flap deflection of approximately 10°, K is a maximum (fig. 11). The change of $\frac{dC_D}{dC_L^2}$ with flap deflection is also plotted in figure 11. Figure 12 is a cross plot of K against $\frac{dC_D}{dC_L^2}$, and the resulting curve is closely approximated by the parabolic equation given.

From figures 6 to 10, it may be seen that

$$C_{L_{max}\ (power\ on)} = C_{L_{max}\ (T_e = 0)} + \frac{K T_e}{qS}$$

where K is a function of flap position. The foregoing equation and the values of K which were obtained from flight tests at relatively low altitudes have been assumed to apply to flight at all altitudes for the purpose of this investigation. It should be realized, however, that in turns made at very high altitudes, the changes in Mach and Reynolds numbers may be large enough to affect the validity of this assumption to a considerable extent.

The variation of $C_{L_{max}}$ with indicated airspeed in the turns was calculated upon the assumption that the maximum rated powers of the engine at 13,000 and 27,000 feet altitude were available. These powers were taken as 900 and 650 brake horsepower, respectively. Using the same propeller characteristics previously applied to the flight-test data for the airplane polars, and an engine revolutions per minute of 2300, curves of thrust against indicated airspeed were computed and are shown in figure 13. The above data were then applied to the formula for $C_{L_{max}\ (power\ on)}$, and the variation of $C_{L_{max}}$ with indicated airspeed was determined for the desired flap, power, and altitude conditions (figs. 14 and 15).

Calculated turns.- The calculated curves of minimum radius of curvature, time to turn 360°, and change of altitude in 360° turns at various speeds are shown in fig-

ures 16 to 21. These curves were determined for an airplane gross weight of 6500 pounds; flap settings of 0°, 22°, and 56°; and for brake horsepowers of 900 and 650 at altitudes of 13,000 and 27,000 feet, respectively. Equations (6), (7), and (8), and data from figures 5, 13, and 14 were used in the computations as indicated by sample calculation A in the appendix.

The radius of curvature and time to turn 360° in horizontal turns were also calculated for various speeds and are shown in figures 22 to 27. The same conditions of weight, flap position, power, and altitude were assumed as in the preceding calculations. For these turns, sample calculation B, involving equations (6), (7), and (9) and data from figures 5 and 13, is given in the appendix.

Test turns.- Results of the flight tests are plotted as points on figures 16 to 27 for the conditions indicated. The test data were reduced to radius of curvature, time to turn 360°, and change of altitude in 360° turns by the use of equations (7), (8), (10), (11), and (12). The flight-path angle θ was determined from the airspeed and change in altitude.

No attempt was made to correct these test points to the conditions of weight, altitude, and brake horsepower used for the calculated turns. In reading the various records made in turns, care was taken to select only those turns or portions of turns during which the desired steady conditions prevailed.

During the course of the tests, it was found that the application of the angular velocity ω obtained from the photographically recorded indications of the directional gyroscope to equation (12) gave the most reliable and consistent results. The test points shown were evaluated on this basis, except for a few cases where directional gyroscope records were not obtained.

Comparison between calculated and test turns.- The test points shown in figures 16 to 21 for the radius of curvature represent the lower boundaries of fields of points obtained in flight. Since it is desired to present only the minimum values for these tests, all of the test points have not been plotted.

Figures 16 to 21 indicate that the calculated minimum radius of curvature represents the actual optimum turning ability of this airplane within close margins. Since the calculated curves were based upon the use of $C_{L_{max}}$, it would be expected that the curves would represent absolute lower boundaries of the radii of curvature. The fact that some of the test points lie below these boundaries is partially due to the deviations from the assumed conditions of weight, altitude, and brake horsepower used in the calculations, as indicated in the description of the tests. This discussion also applies to the calculated and measured values of the time to turn 360°, the agreement between them being similar to that for the radii of curvature. Also shown on figures 16 to 21 are curves of calculated radius of curvature computed on a basis of $C_{L_{max}}$ for $T_e = 0$ (neglecting the effect of thrust on $C_{L_{max}}$) for each of the flap conditions. These curves indicate that this method is too conservative for estimating the minimum radius of curvature, especially in the low-speed region, and that the effect of thrust on $C_{L_{max}}$ should be considered. For the change of altitude in 360° turns, there is a greater scatter among the test points and a greater deviation from the calculated curves; however, the curves indicate satisfactorily the relative effects of flap deflections and altitude on the loss of altitude in turns.

The test points for horizontal turns, plotted on figures 22 to 27, represent all turns in which the desired steady conditions prevailed, and there was no noticeable change of altitude. It should be pointed out that the test points do not represent boundaries of a field of test points, as was the case for turns at nearly $C_{L_{max}}$. In addition to the curves which were computed on a basis of 900 and 650 brake horsepower, curves are shown on figures 22 and 25 for computations based on 800 and 600 brake horsepower, respectively. These curves illustrate the effect of a reduction of power. Thrust curves for these lower powers are shown on figure 13.

As the speed at which horizontal turns are flown at constant horsepower is reduced, the lift coefficient increases until a speed is reached at which C_L is a maximum for that speed. Thus, in figure 22, for 900 brake

horsepower this speed is 113.5 miles per hour. Figure 16 also shows this speed as the zero loss of altitude turn at $C_{L_{max}}$ for the given conditions. Any turn, even at $C_{L_{max}}$, for this brake horsepower and at a speed below 113.5 miles per hour would be a climbing turn. To fly horizontal turns at a lower speed would require a decrease in power, and the portions of the curves for speeds below these critical speeds in figures 22 to 25 have been computed on the basis of this decreasing power required. For the conditions of figures 26 and 27, as speed is reduced the minimum speed for level flight (infinite radius horizontal turn) is reached before the lift coefficient becomes a maximum, and hence it is not possible to fly a horizontal turn at $C_{L_{max}}$ for these conditions.

The test points and the calculated curves for the radius of curvature in horizontal flight at 13,000 feet altitude for the various flap conditions are in close agreement, as shown in figures 22, 23, and 24.

The horizontal turns at 27,000 feet altitude (figs. 25, 26, and 27) show greater scatter of the test points, especially for the flaps-deflected (high drag) conditions. At these conditions and where the airplane approached its ceiling, the effects of slight changes of power output, or of unsteady atmospheric conditions, were accentuated. Small changes of angle of bank in similar turns, while giving no noticeable lateral acceleration, had a large effect upon the radius of curvature, as did slight variations of piloting technique. It is also possible that at this altitude the actual lift and drag characteristics of the airplane varied somewhat from the lift and drag characteristics obtained at lower altitudes due to the difference in Mach numbers for the different altitudes. Despite the scatter of the test points, the calculated curves for figures 25 and 26 represent closely the mean curves through the test points and hence may be considered indicative of the performance of the airplane. For the flaps 56° down condition (fig. 27) there was a relatively small amount of power available for maneuvering, and the effects of the above-mentioned difficulties were so great that it was impossible to obtain consistent test points establishing the turning performance or verifying the calculations.

The time to turn 360° in horizontal flight (figs. 22 to 27), as shown both by the test points and the calculated curves, varies in a manner similar to that for the corresponding value of radius of curvature, since in equation (7) $\cos \theta = 1$ for horizontal turns.

Airplane turning performance as affected by flaps and altitude.- The calculated curves will be used as the basis for further discussion. These curves are preferred since they are based on standard conditions of weight, altitude, and power output; whereas, curves that might have been drawn through the test points would have represented somewhat variable conditions.

An examination of figures 16 to 21 shows that for each of the specified condtions, the minimum radius of curvature is practically constant for indicated airspeeds above 100 miles per hour at 13,000 feet altitude and above 110 miles per hour at 27,000 feet altitude. The time to turn 360° decreases as speed increases, but at a sacrifice of altitude. This loss of altitude in 360° turns varies approximately linearly with the airspeed, and for the same density altitude the curves for the different flap deflections are nearly parallel.

Comparing the results for the various flap deflections at 13,000 feet altitude (figs. 16, 17, and 18), an increase of flap deflection results in a decrease of the minimum radius of curvature and the time to turn 360°, but with an additional sacrifice of altitude. The initial 22° flap deflection has a greater effect than the additional 34° deflection which produces the 56° down condition. At 27,000 feet altitude (figs. 19, 20, and 21), the same relationships between flap conditions apply but, for a given flap setting, the absolute values of radius, time, and change in altitude are greater at the higher altitude. Examining equation (6), this increase in radius is seen to be due to the decrease in air density and to the small effect of changes in $C_{L_{max}}$ and θ brought about by the decreased horsepower.

In the horizontal turns at 13,000 feet altitude (figs. 22, 23, and 24), there is for each flap deflection a horizontal turn, of minimum radius when the airplane is flying at $C_{L_{max}}$. This minimum radius and the speed at which it occurs decrease with increasing flap deflection.

As previously explained, the radii of curvature for speeds below these critical speeds were computed on the basis of reducing power to maintain the turns horizontal. Actually, it would no doubt be preferable at these lower speeds to fly climbing turns at the stall boundary curves of figures 15, 16, and 17. At any speed above about 112 miles per hour, the radius for the flaps-up condition is smaller than that for each of the flaps-deflected conditions. Above 123 miles per hour the radius increases with an increase in flap deflection, and the advantage of having the flaps up increases with speed. As previously noted for the horizontal turns, the time to turn 360° varies with speed in a manner similar to the radius.

For the horizontal turns at 27,000 feet altitude, (figs. 25, 26, and 27), the flaps-up condition appears to be the optimum. It is seen that the horizontal turn of minimum radius no longer occurs at the speed where C_L reaches the maximum, but at some higher speed. As previously mentioned, $C_{L_{max}}$ cannot be reached in horizontal turns for the flaps-down 22° and 56° conditions at this altitude and, as flap deflection is increased, the speed range over which horizontal turns may be flown is considerably decreased. For a given speed the radius of curvature is always less with flaps up (fig. 25) than with flaps down (figs. 26 and 27). A comparison of values of the radius of curvature for flaps 56° down with those for flaps 22° down shows that the minimum radius horizontal turn is slightly smaller for the 56° setting, and the radius is smaller at each speed below 97 miles per hour. At higher speeds the radius increases rapidly and is greatest for the 56° setting. Compared to the horizontal turns at 13,000 feet, those at 27,000 feet for the same flap position show a much greater radius, due not only to the decrease in air density, but also to the lower brake horsepower. Analysis shows that flaps can decrease the radii of horizontal turns only if, over the range of drag coefficients considered, the corresponding lift coefficients are greater with the flaps deflected.

Airplane turning performance as affected by weight.- Due to the fact that the gross weight of the airplane could not be varied conveniently over a wide range, no flight tests were made to study the effect of weight on the turning performance; however, figures 28 to 31 show the computed effect of an increase and a decrease of 1000

pounds in airplane gross weight. The curves in these figures for the standard airplane weight of 6500 pounds have been taken from figures 16, 19, 22, and 25.

As would be expected from equation (6), these changes of weight cause a corresponding substantial change of radius of curvature and time to turn 360° in turns at $C_{L_{max}}$ (figs. 28 and 29). The effects of the changes of radius of curvature and flight-path angle are such that little difference in loss of altitude in 360° turns occurs.

For most horizontal turns, C_L is less than maximum and hence, as may be seen from an examination of the term $\frac{C_L qS}{W}$ in equation (6), a given change of weight has a greater percentage effect on radius of curvature than for turns at $C_{L_{max}}$. This is especially evident in the horizontal turns at 27,000 feet altitude (fig. 31).

Turning-performance diagrams.- For convenience, turning-performance diagrams for each flap and altitude condition for this airplane are presented in figures 32 to 37 in the form used in references 3 and 4. Information concerning any turn within the limits and ranges of these diagrams may thus be found. These data are also presented in figures 38 and 39 in the more general form of reference 5. The method by which figures 38 and 39 were computed conformed in general with the method of reference 5, with the exception that the effect of thrust on $C_{L_{max}}$ was considered. Sample calculation A in the appendix partially illustrates the methods used to obtain figures 32 to 39.

CONCLUSIONS

In general:

1. The turning performance of an airplane can be calculated with satisfactory accuracy by the methods of this report, provided the airplane polar and thrust curves are available for the specified conditions.

2. The effect of thrust on the maximum lift coefficient should be considered in predicting the turning performance of an airplane, especially in the low-speed region.

For turns flown at a given altitude at nearly maximum lift coefficient with the Navy F2A-3 airplane:

3. The radius of curvature and time to turn 360° at a given speed decreases as the flap deflection is increased.

4. The radius of curvature for a given flap deflection is a nearly constant minimum over a wide range of speed.

5. The loss of altitude in 360° turns increases as the flap deflection is increased, and the difference of this loss of altitude for any two flap deflections is approximately constant over the speed range considered (90 to 160 miles per hour).

6. The loss of altitude in 360° turns for a given flap deflection varies approximately linearly with airspeed over the speed range considered.

7. For the flap deflections considered in this report, the effect of the first 22° of flap deflection on turning performance is greater than the additional effect of the last 34°.

8. The turning performance is poorer at the higher altitudes, due chiefly to the direct effect of decreasing air density.

9. An increase in the airplane gross weight results in an increase in the radius of curvature and the time to turn 360°. The change of altitude during a 360° turn is affected but little by changes in weight.

For horizontal turns flown at 13,000 feet altitude with the Navy F2A-3 airplane:

10. For each flap deflection there is a speed at which the radius of curvature is a minimum, and for this turn the airplane is being flown at the maximum lift coefficient.

11. The minimum radius of curvature and the speed at which it occurs decrease as the flap deflection is increased.

12. At any airspeed above 112 miles per hour the radius of curvature is a minimum with flaps up, and this advantage over the other flap deflections increases with airspeed.

For horizontal turns at 27,000 feet altitude with the Navy F2A-3 airplane:

13. For each flap deflection there is a speed at which the radius of curvature is a minimum, but for this turn the airplane is not being flown at the maximum lift coefficient.

14. The maximum lift coefficient cannot be reached in horizontal turns for the flaps 22° and 56° deflected conditions.

15. At any speed the radius of curvature is a minimum for the flaps-up condition.

16. The turning performance is inferior to that for horizontal turns at 13,000 feet altitude, due to the direct effect of decreased air density and to the reduced power output.

17. A change of the airplane gross weight has a large effect on the turning performance, and a decrease of weight would result in greatly improved performance.

Ames Aeronautical Laboratory,
National Advisory Committee for Aeronautics,
Moffett Field, Calif.

APPENDIX

SAMPLE CALCULATIONS

Example A.- The sample calculations are carried out for the following conditions:

Speed . . . . . 120 miles per hour

Weight . . . . . 6,500 pounds

Lift coefficient . . $C_{L_{max}}$

Wing area . . . . . 208.9 square feet

Flaps . . . . . Up

Density altitude. . . 13,000

σ 0.672

Power . . . . . 900 brake horsepower

(The point for which computations are made is plotted in figure 16)

The steps required for the computation of the turning performance are as follows:

1. From figure 14, for flaps up at 120 miles per hour

$$C_{L_t} = C_{L_{max}} = 1.71$$

2. From figure 5, for flaps up at $C_L = 1.71$

$$C_{D_t} = 0.235$$

3. The drag in the turn

$$D_t = C_{D_t} qS$$

$$D_t = (0.235)\ (0.00255)\ (120)^2\ (208.9)$$

$$D_t = 1812 \text{ pounds}$$

4. From figure 13, with 900 brake horsepower at 13,000 feet altitude, for 120 miles per hour

$$T_e = 1635 \text{ pounds}$$

5. $$\sin\theta = \frac{T_e - D_t}{W}$$

$$\sin\theta = \frac{1635 - 1812}{6500} = -0.0273$$

$$\theta = -1.6^\circ$$

$$\cos\theta = 0.9996$$

6. The radius of curvature

$$R = \frac{(1.47)^2 V_i^2}{\sigma g\left[\left(\frac{C_L qS}{W}\right)^2 - \cos^2\theta\right]^{1/2}}$$

$$R = \frac{(1.47)^2 (120)^2}{(0.672)(32.2)\left\{\left[\frac{(1.71)(0.0255)(120)^2(208.9)}{6500}\right]^2 - (0.9996)^2\right\}^{1/2}}$$

$$R = 818 \text{ feet}$$

7. Time to turn 360°

$$t = \frac{2\pi R \sigma^{1/2} \cos\theta}{1.47 V_i}$$

$$t = \frac{(2)(3.14)(818)(0.672)^{1/2}(0.9996)}{(1.47)(120)} = 23.9 \text{ seconds}$$

8. The change in altitude in a 360° turn

$$\Delta H = 2\pi R \sin\theta \cos\theta$$

$$\Delta H = (2)(3.14)(818)(-0.0273)(0.9996) = -141 \text{ feet}$$

The computations made in order to present the data in the form of the turning-performance diagram of figure 32 are shown in the following steps:

9. The lift coefficient in straight flight

$$C_{L_l} = \frac{W \cos \theta_o}{qS}$$

Since $\cos \theta_o$ is practically unity in the range considered

$$C_{L_l} = \frac{(6500)}{(0.00255)(120)^2(208.9)} = 0.84$$

10. From figure 5, for $C_L = 0.84$

$$C_{D_l} = 0.080$$

11. The drag in straight flight

$$D_l = C_{D_l} qS$$

$$D_l = (0.080)(0.00255)(120)^2(208.9) = 615 \text{ pounds}$$

12. $$\sin \theta_o = \frac{T_e - D_l}{W}$$

$$\sin \theta_o = \frac{1635 - 615}{6500} = 0.157$$

$\theta_o = 9.0^\circ$ (ordinate of angle of straight-climb curve)

13. $\theta_o - \theta = 9.0 - (-1.6) = 10.6^\circ$ (ordinate of stall boundary curve)

The computations made in order to present the data in the form of the turning-performance diagram of figure 38 are shown in the following steps:

14. From figure 5, for flaps up

$$\frac{dC_D}{dC_L^2} = 0.070$$

15. The span loading

$$l_s = \pi \frac{W}{S} \frac{dC_D}{dC_L^2}$$

$$l_s = \frac{(3.14)(6500)(0.070)}{208.9} = 6.84$$

16. $$\gamma = \frac{(T_e - D_l)}{W} \frac{1}{l_s} = \frac{\sin \theta_o}{l_s}$$

$$\gamma = \frac{0.157}{6.84} = 0.0230$$

17. $$\Delta\gamma = \frac{(D_t - D_l)}{W} \frac{1}{l_s}$$

$$\Delta\gamma = \frac{(1812 - 615)}{(6500)(6.84)} = 0.0269$$

Example B.- Steps required for the computation of the radius of curvature and time to turn 360° for a horizontal turn are as follows. (The conditions are the same as in Example A except for the value of C_L. The point for which computations are made is plotted in figure 22.)

1. $T_e = C_{D_t} qS$

$$C_{D_t} = \frac{T_e}{qS}$$

$$C_{D_t} = \frac{1635}{(0.00255)(120)^2(208.9)} = 0.213$$

2. From figure 5, for flaps up at $C_D = 0.213$

$$C_{L_t} = 1.63$$

3. The radius of curvature

$$R = \frac{(1.47)^2 V_i^2}{\sigma g \left[\left(\frac{C_L \, qS}{W} \right)^2 - \cos^2 \theta \right]^{1/2}}$$

$$R = \frac{(1.47)^2 (120)^2}{(0.672)(32.2)\left\{ \left[\frac{(1.63)(0.00255)(120)^2 (208.9)}{(6500)} - 1 \right] \right\}^{1/2}}$$

$$R = 877 \text{ feet}$$

4. The time to turn 360°

$$t = \frac{2 \pi R \sigma^{1/2} \cos \theta}{1.47 \, V_i}$$

$$t = \frac{(2)(3.14)(892)(0.672)^{1/2}(1)}{(1.47)(120)} = 25.4 \text{ seconds}$$

REFERENCES

1. Bierman, David, and Hartman, Edwin P.: Tests of Five Full-Scale Propellers in the Presence of a Radial and a Liquid-Cooled Engine Nacelle, Including Tests of Two Spinners. Rep. No. 642, NACA, 1938.

2. Diehl, Walter S.: Some Fundamental Considerations in Regard to the Use of Power in Landing an Airplane. T.N. No. 692, NACA, 1939.

3. Gates, S. B.: Notes on the Dogfight. Rep. No. B.A. 1613, British R.A.E., 1940.

4. Morgan, M. B., and Morris, D. E.: Notes on the Turning Performance of the Spitfire as Affected by Altitude and Flaps. Rep. No. B.A. 1668, British R.A.E., 1941.

5. Wetmore, J. W.: Study of Turning Performance of a Fighter-Type Airplane Particularly as Affected by Flaps and Increased Supercharging. NACA, A.C.R., June 1942.

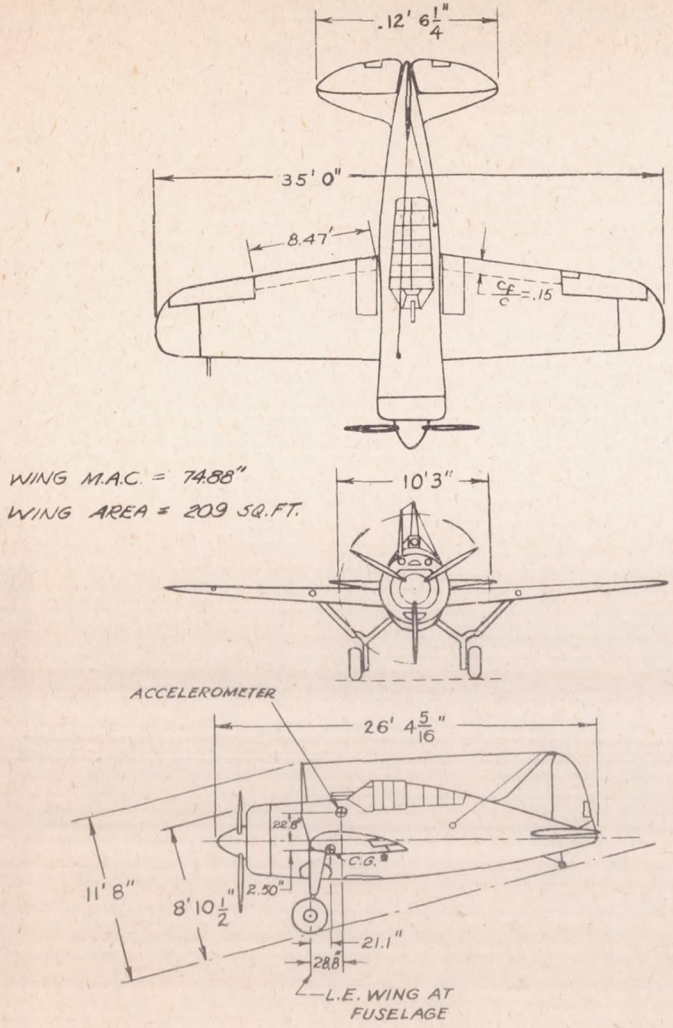

*POSITION AS TESTED IN FLIGHT (WHEELS DOWN)

Figure 1. Navy F2A-3 airplane, three-view drawing.

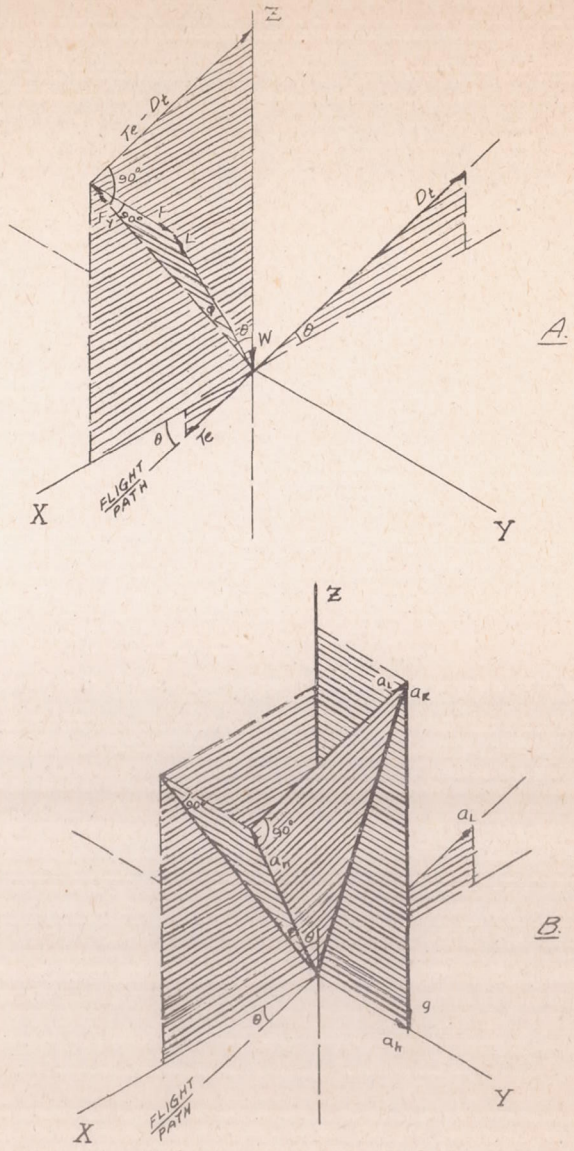

FIGURE 4 - FORCE AND ACCELERATION VECTOR DIAGRAMS FOR AN AIRPLANE IN STEADY TURNING FLIGHT.

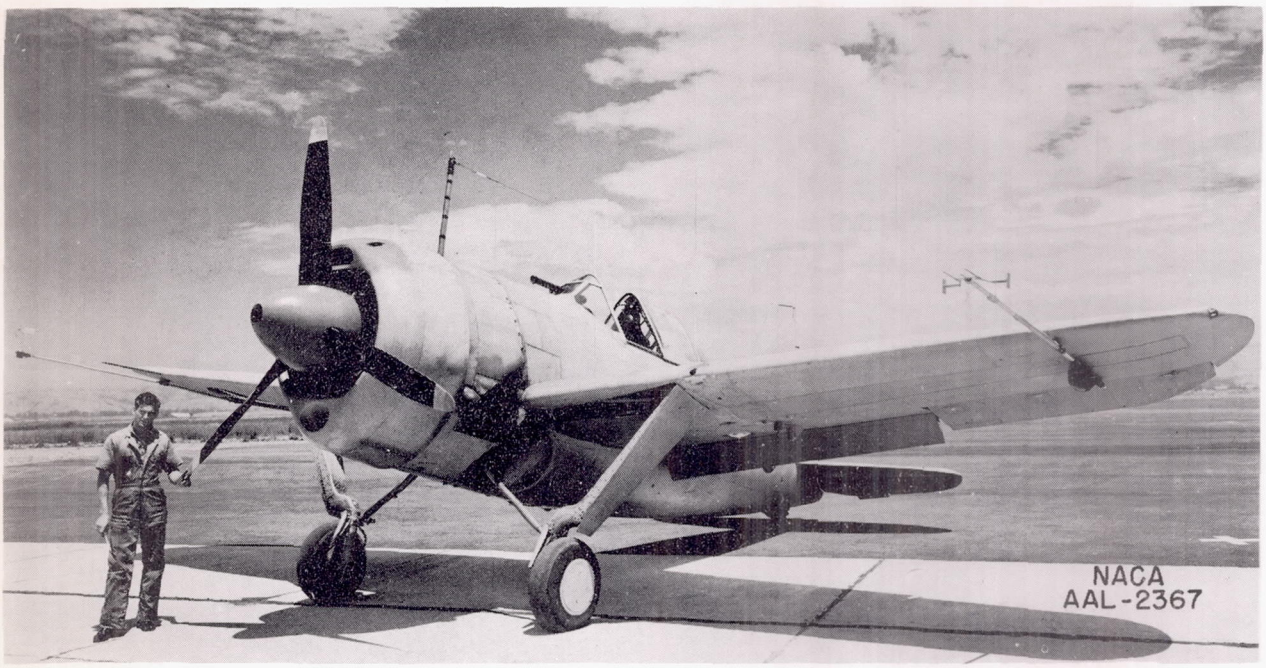

Figure 2.- Three-quarter front view of Navy F2A-3 airplane as instrumented for tests, flaps down.

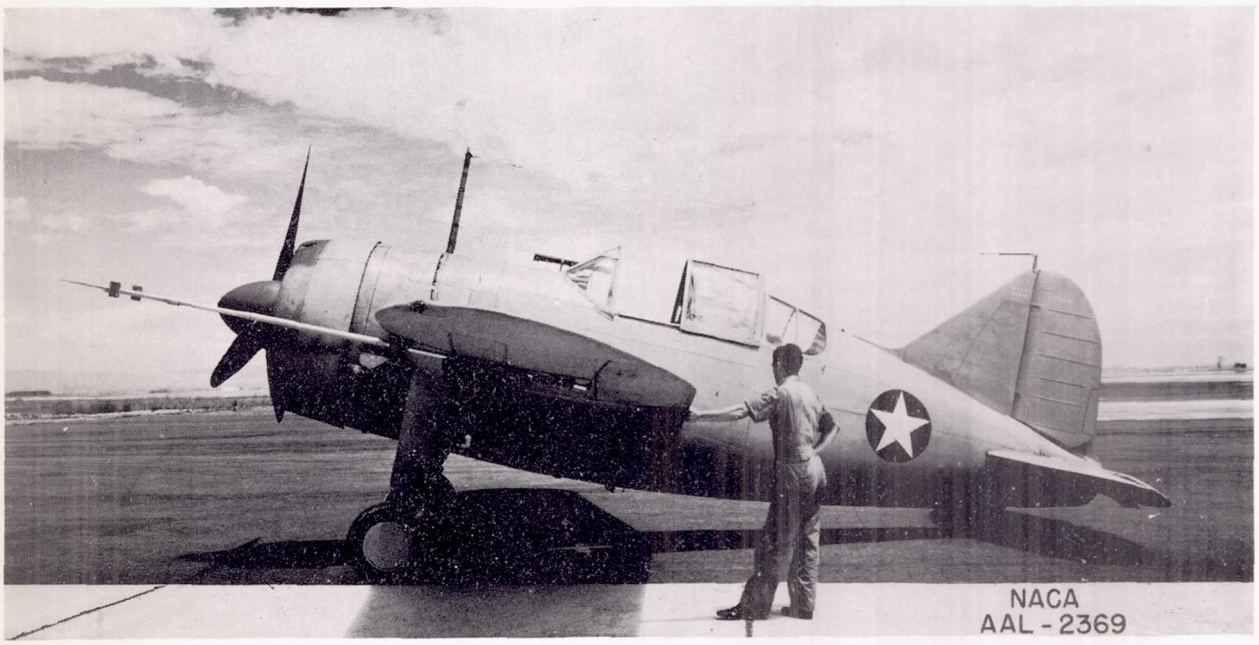

Figure 3.- Side view of Navy F2A-3 airplane as instrumented for tests, flaps down.

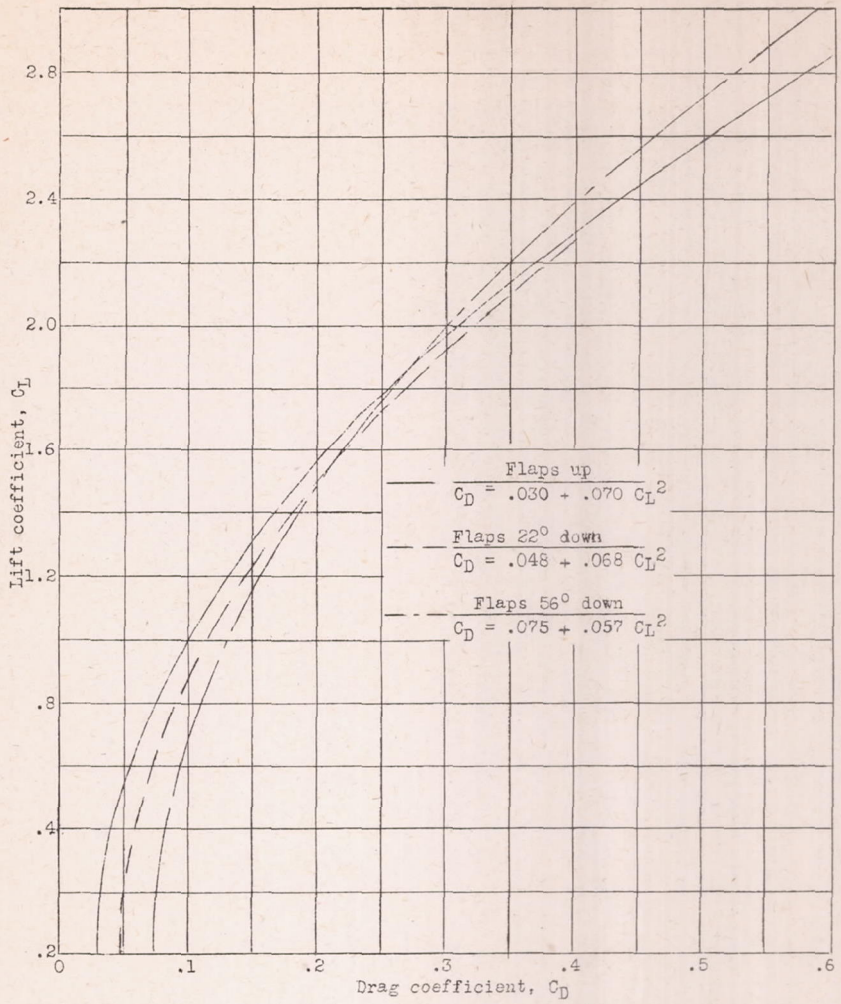

Figure 5.- Variations of lift coefficient with drag coefficient for various flap positions, Navy F2A-3 airplane.

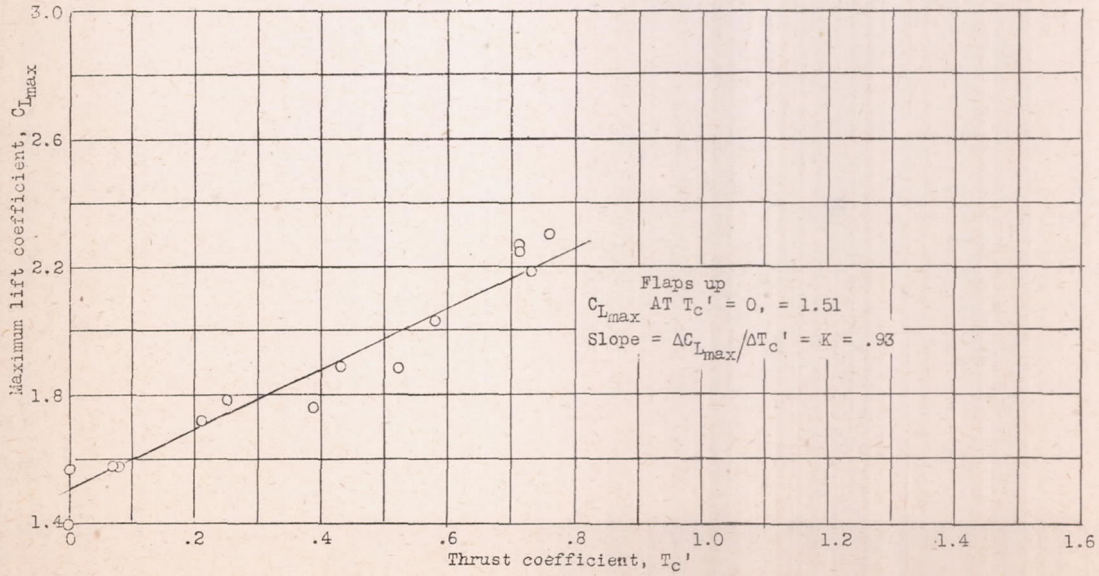

Figure 6.- Variation of maximum lift coefficient with thrust coefficient, flaps up, Navy F2A-3 airplane.

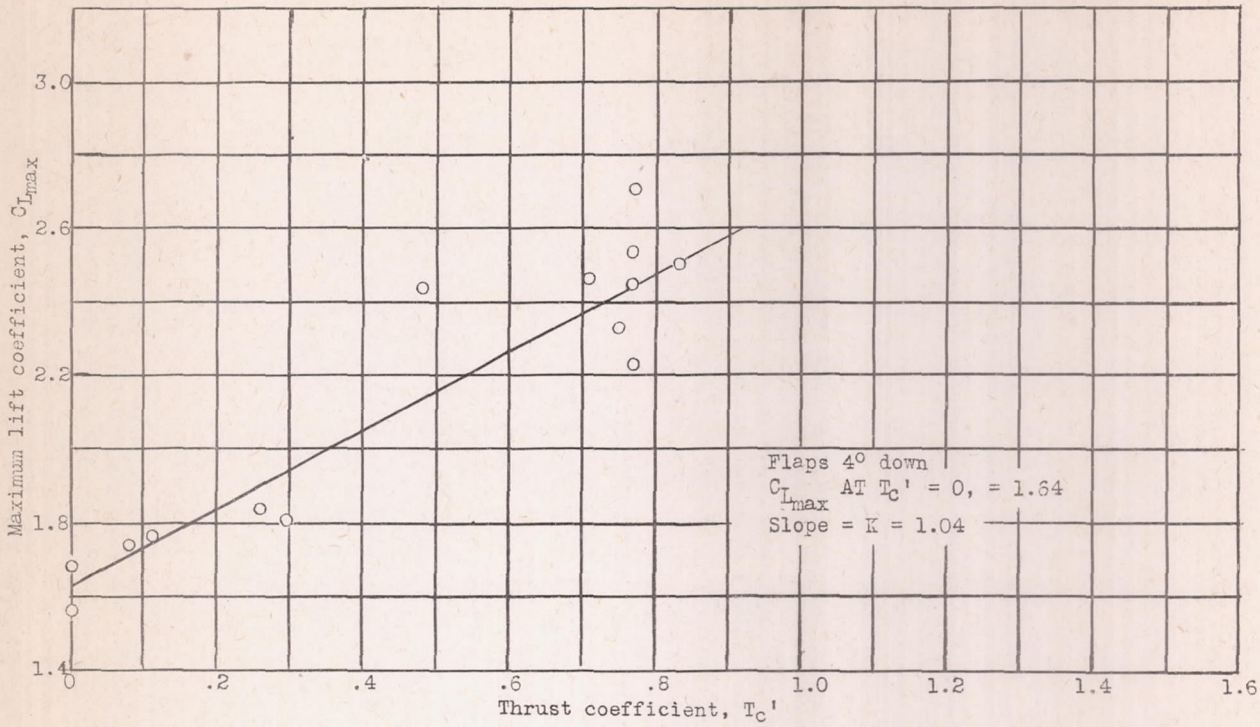

Figure 7.- Variation of maximum lift coefficient with thrust coefficient, flaps 4° down, Navy F2A-3 airplane.

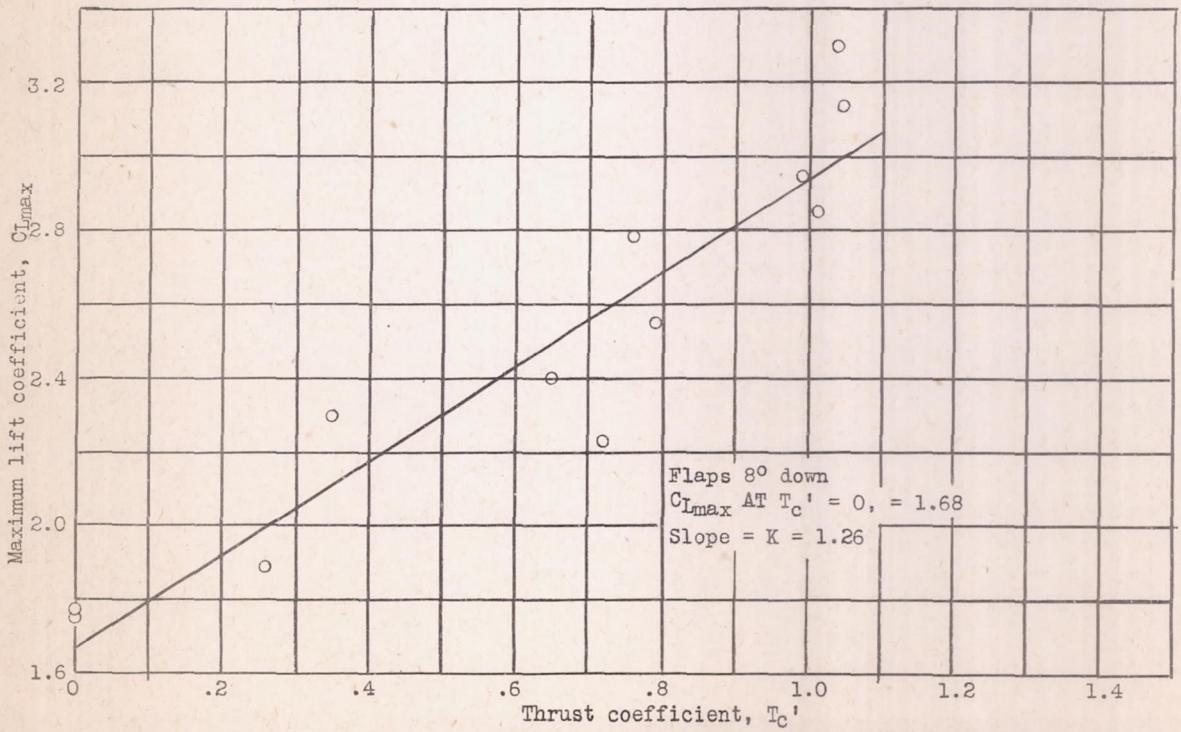

Figure 8.- Variation of maximum lift coefficient with thrust coefficient, flaps 8° down, Navy F2A-3 airplane.

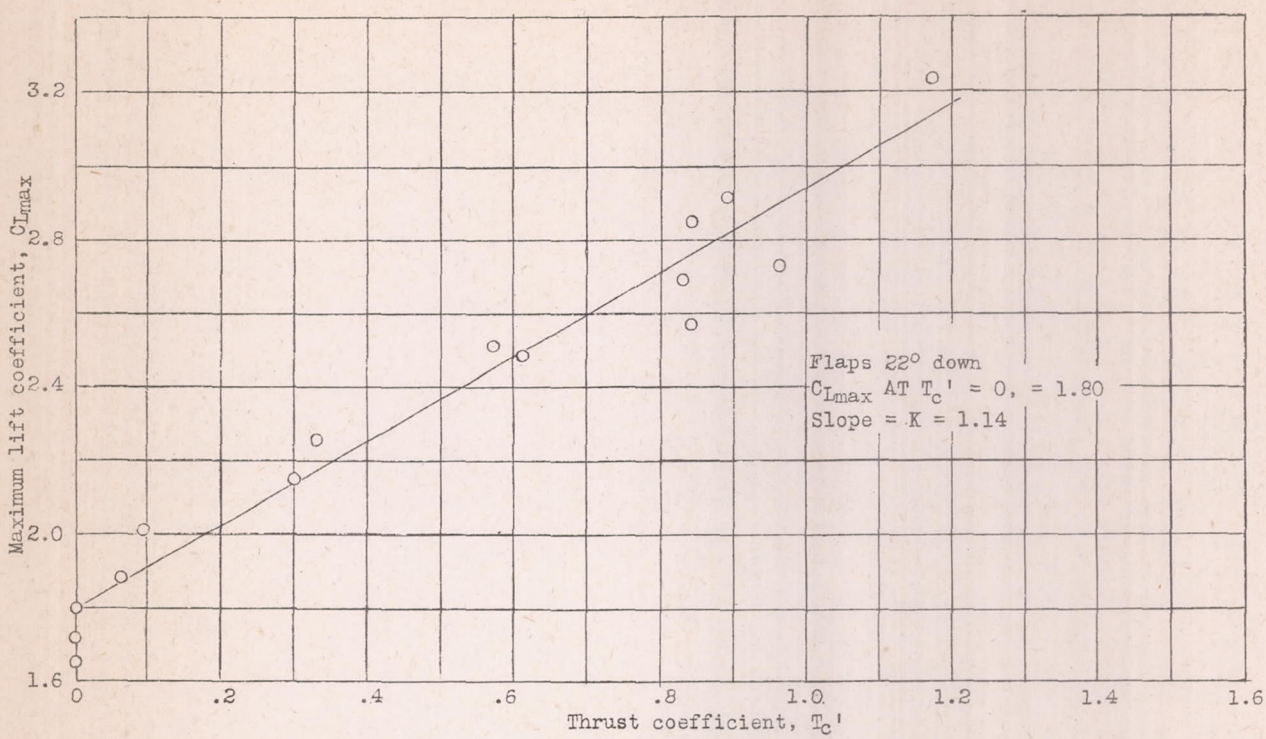

Figure 9.- Variation of maximum lift coefficient with thrust coefficient, flaps 22° down, Navy F2A-3 airplane.

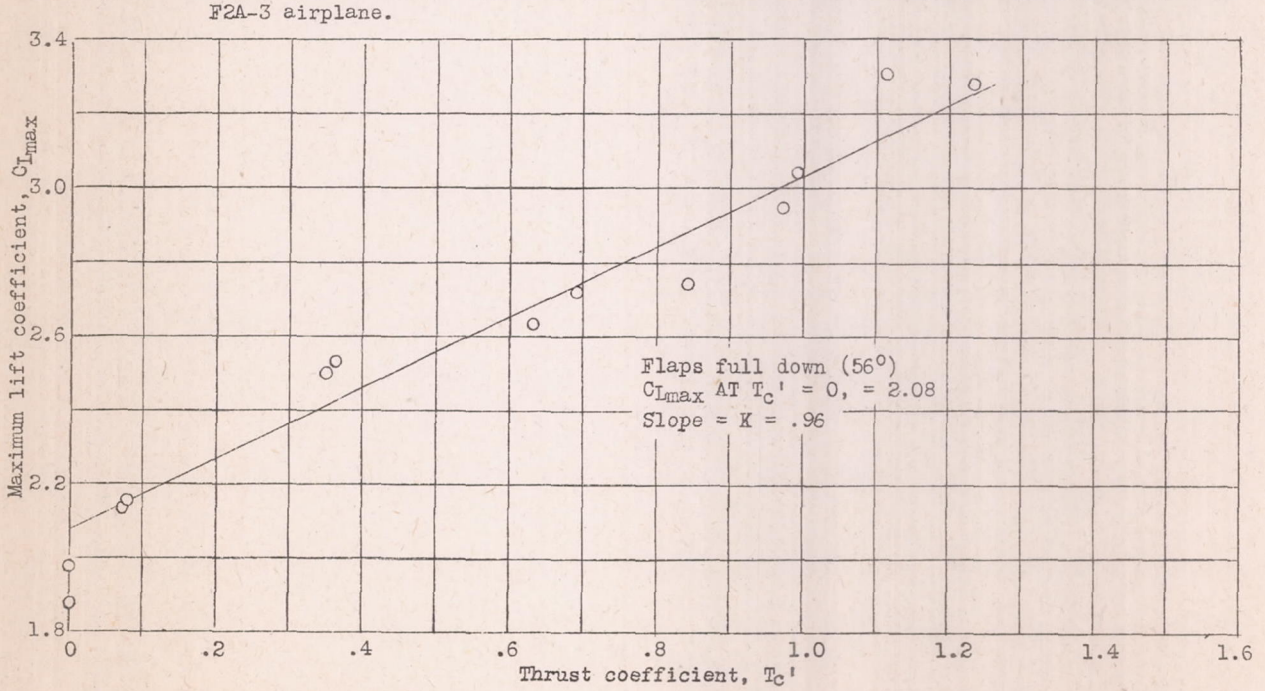

Figure 10.- Variation of maximum lift coefficient with thrust coefficient, flaps 56° down, Navy F2A-3 airplane.

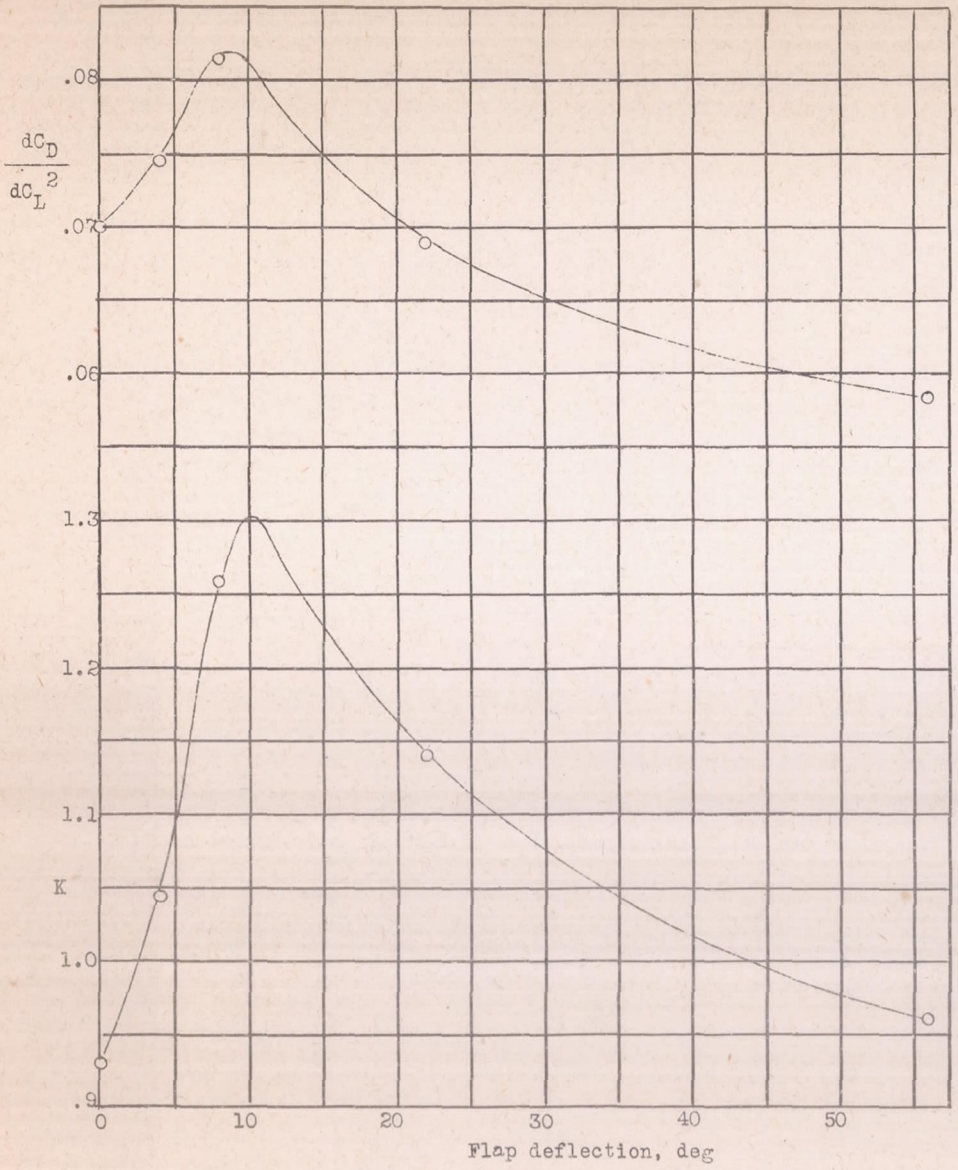

Figure 11.- Variation of K and dC_D/dC_L^2 with flap deflection, Navy F2A-3 Airplane.

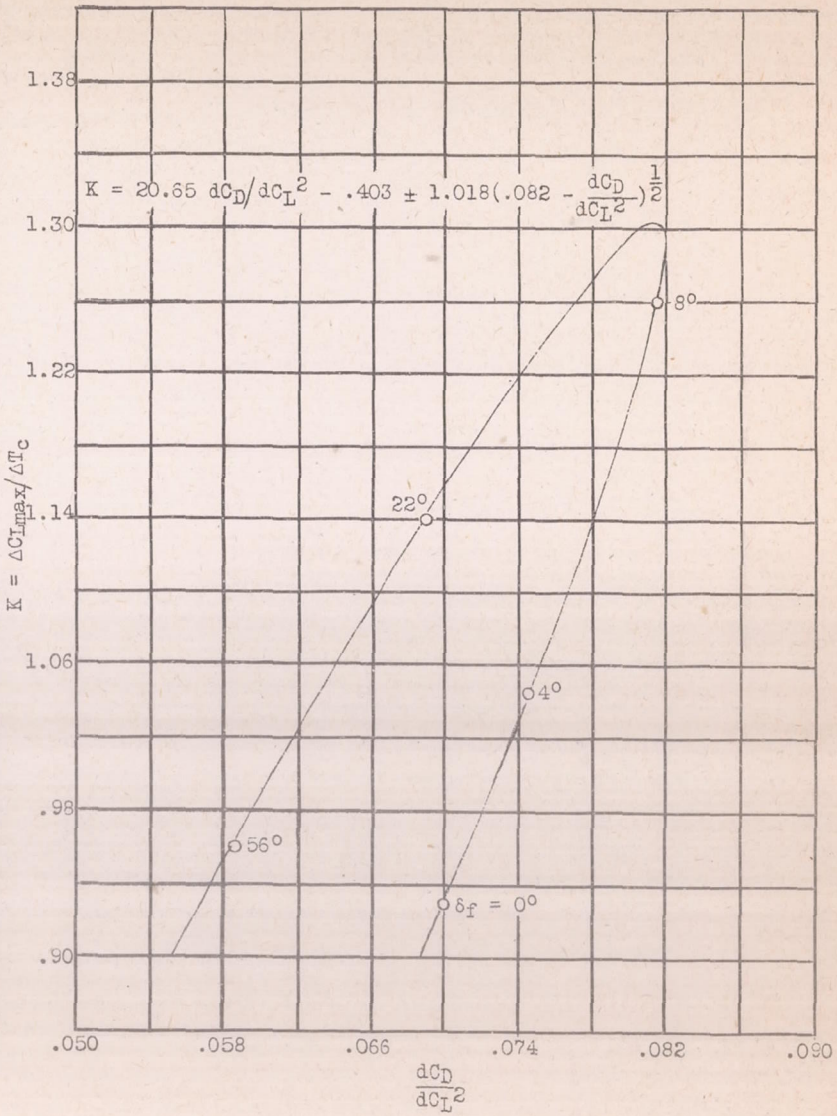

Figure 12.- Variation of K with dC_D/dC_L^2, Navy F2A-3 airplane.

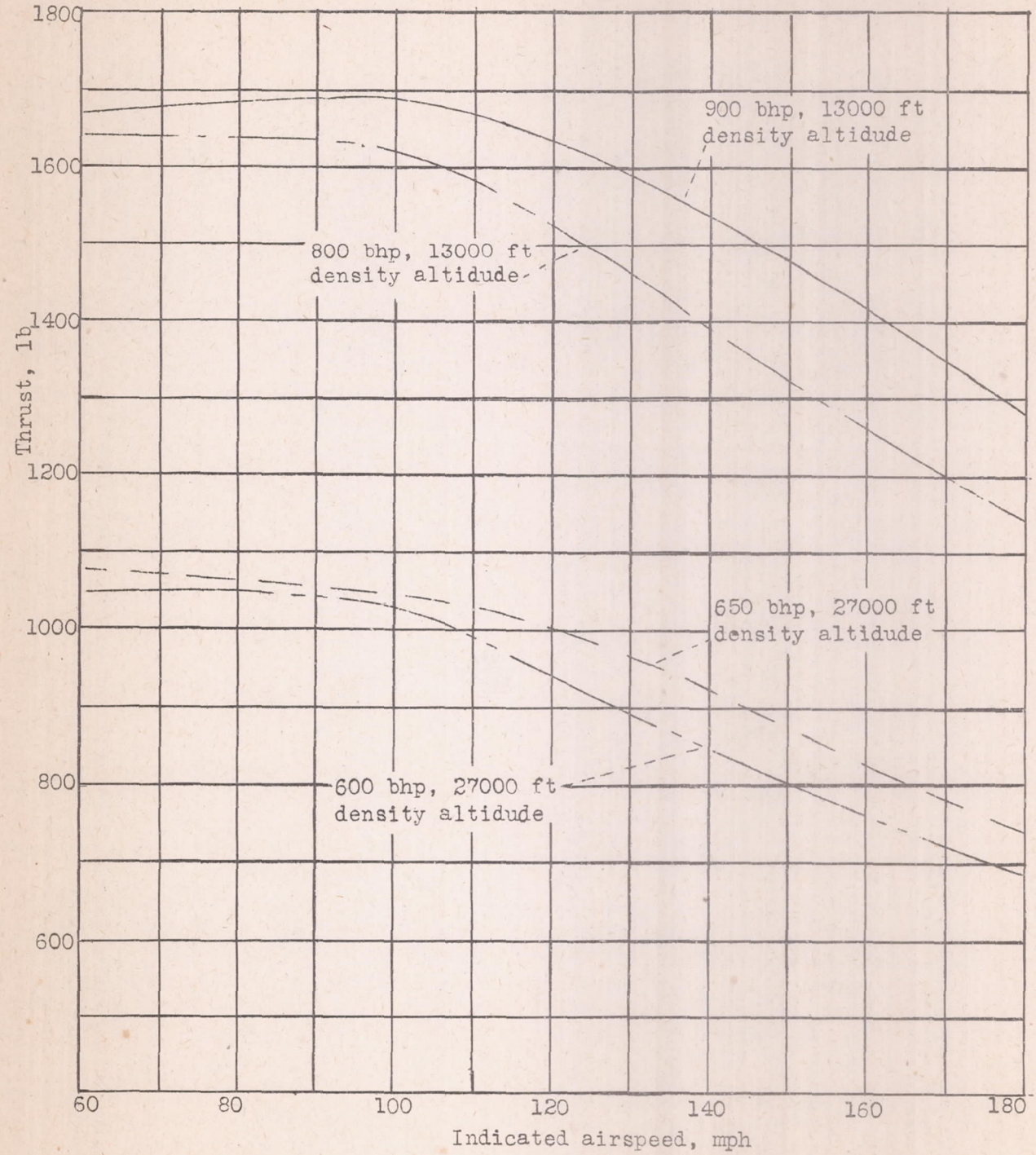

Figure 13.- Variation of thrust with indicated airspeed for various altitudes and horsepowers at 2300 rpm, Navy F2A-3 airplane.

(1 block = 10 divisions on 1/32 Arch. scale)

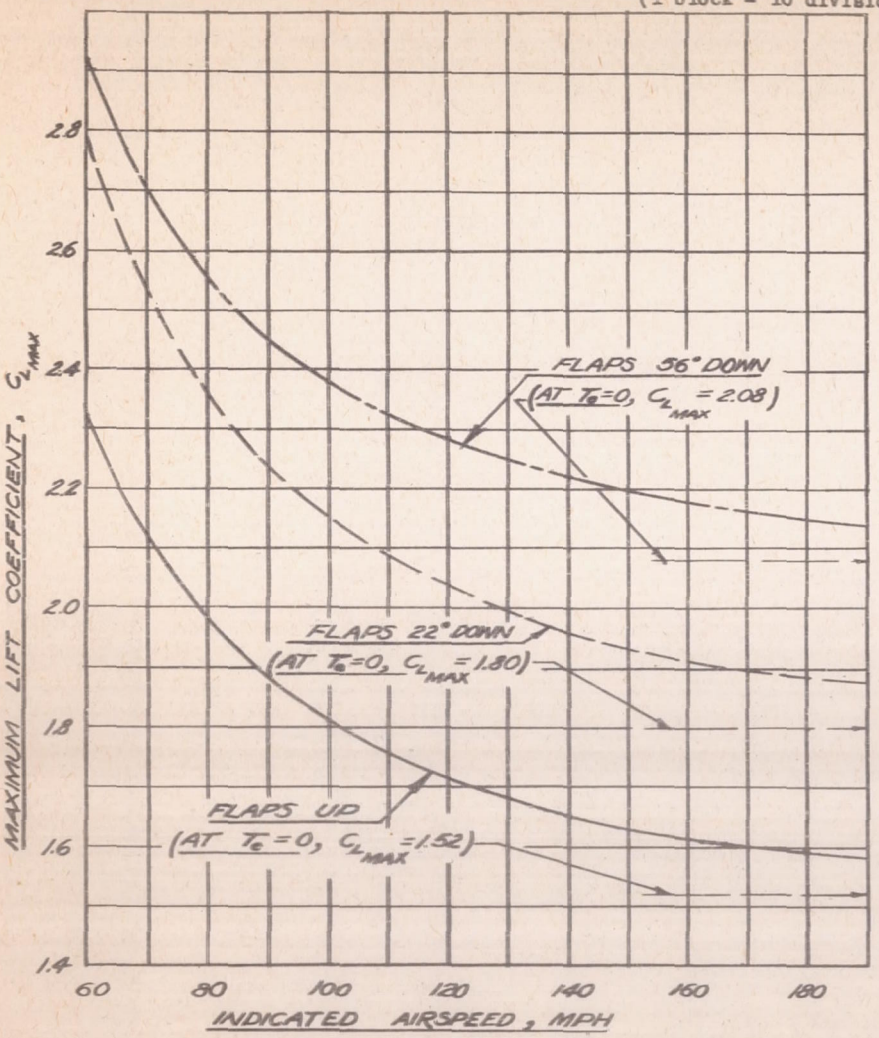

FIGURE 14.-VARIATION OF MAXIMUM LIFT COEFFICIENT WITH INDICATED AIRSPEED FOR VARIOUS FLAP POSITIONS, 13000 FEET ALTITUDE, 900 HORSEPOWER, NAVY F2A-3 AIRPLANE

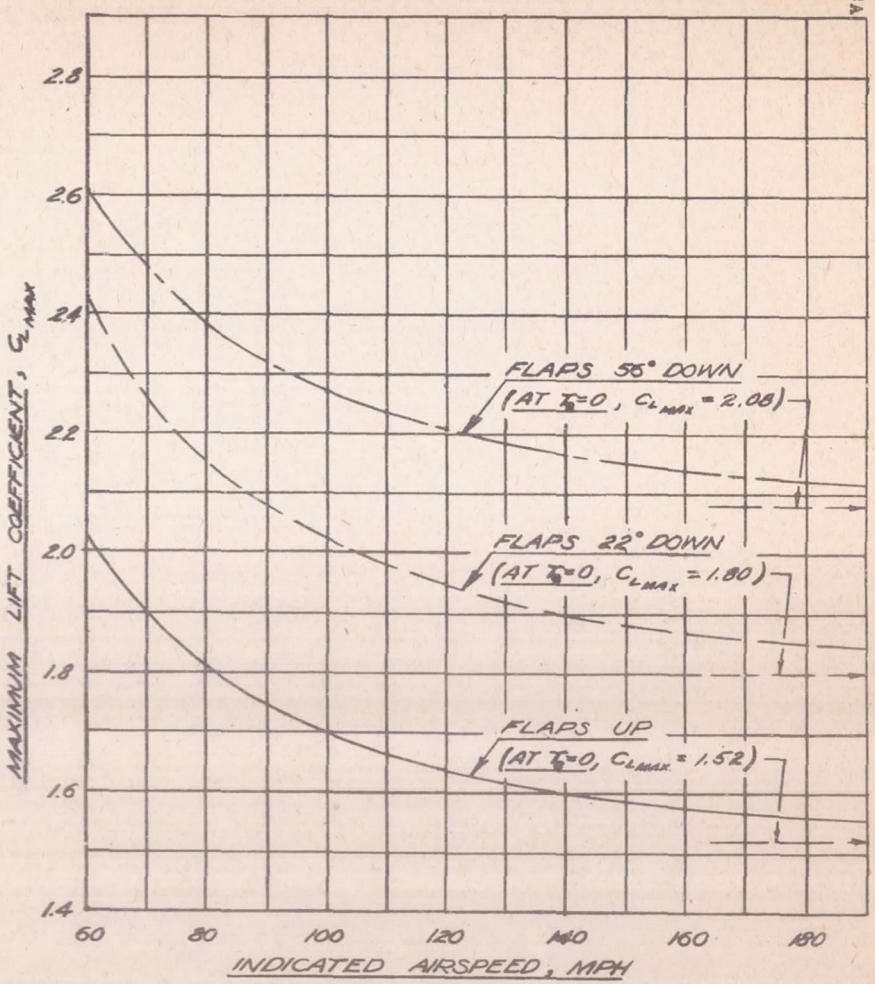

FIGURE 15.-VARIATION OF MAXIMUM LIFT COEFFICIENT WITH INDICATED AIRSPEED FOR VARIOUS FLAP POSITION, 27000 FEET ALTITUDE, 650 HORSEPOWER, NAVY F2A-3 AIRPLANE.

NACA

(1 block = 10/32")

Fig. 16

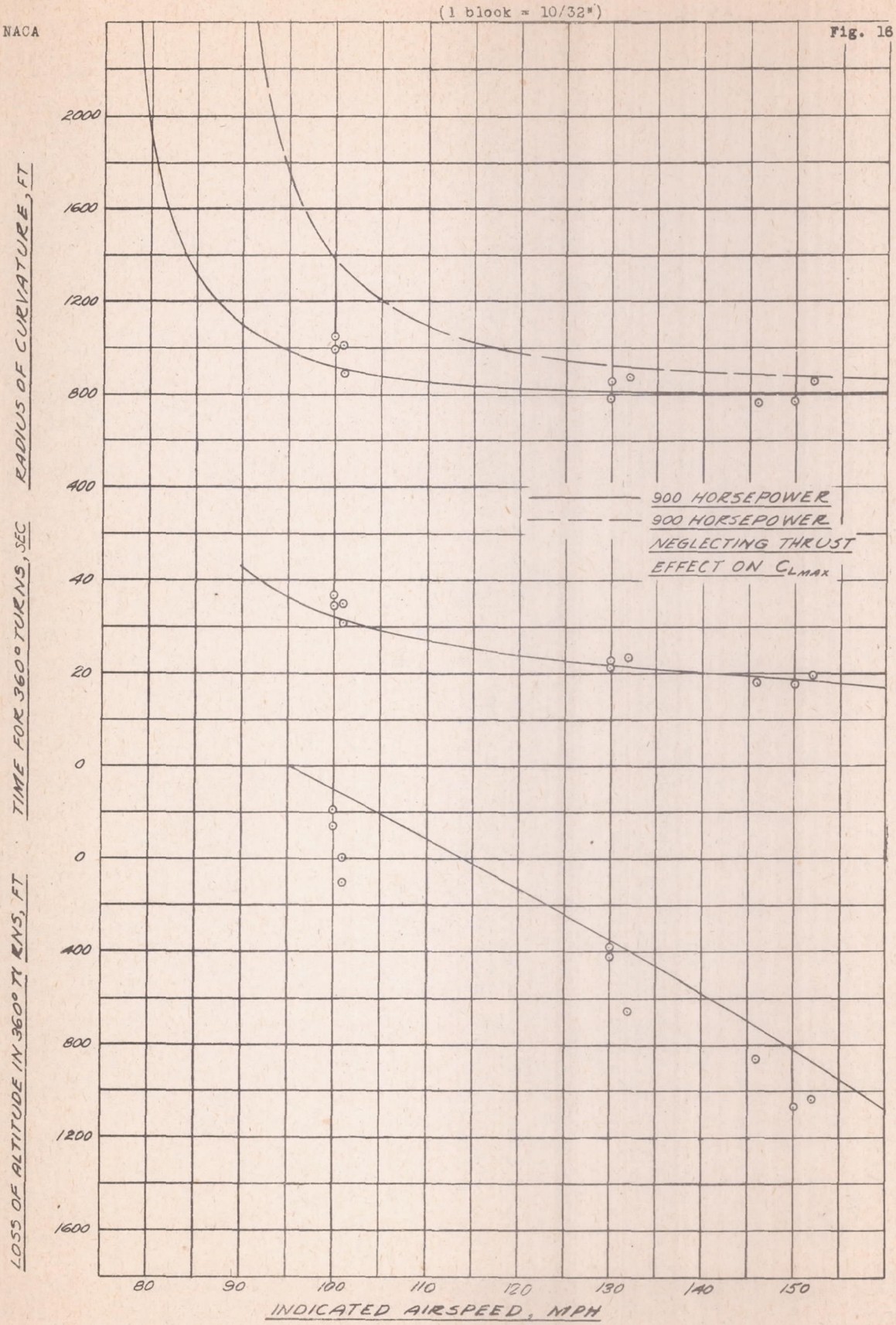

FIGURE 16.- CALCULATED AND EXPERIMENTAL DETERMINATIONS OF THE TURNING PERFORMANCE, IN STEADY TURNS, AT 13000 FEET ALTITUDE, MAXIMUM LIFT COEFFICIENT, FLAPS UP, NAVY F2A-3

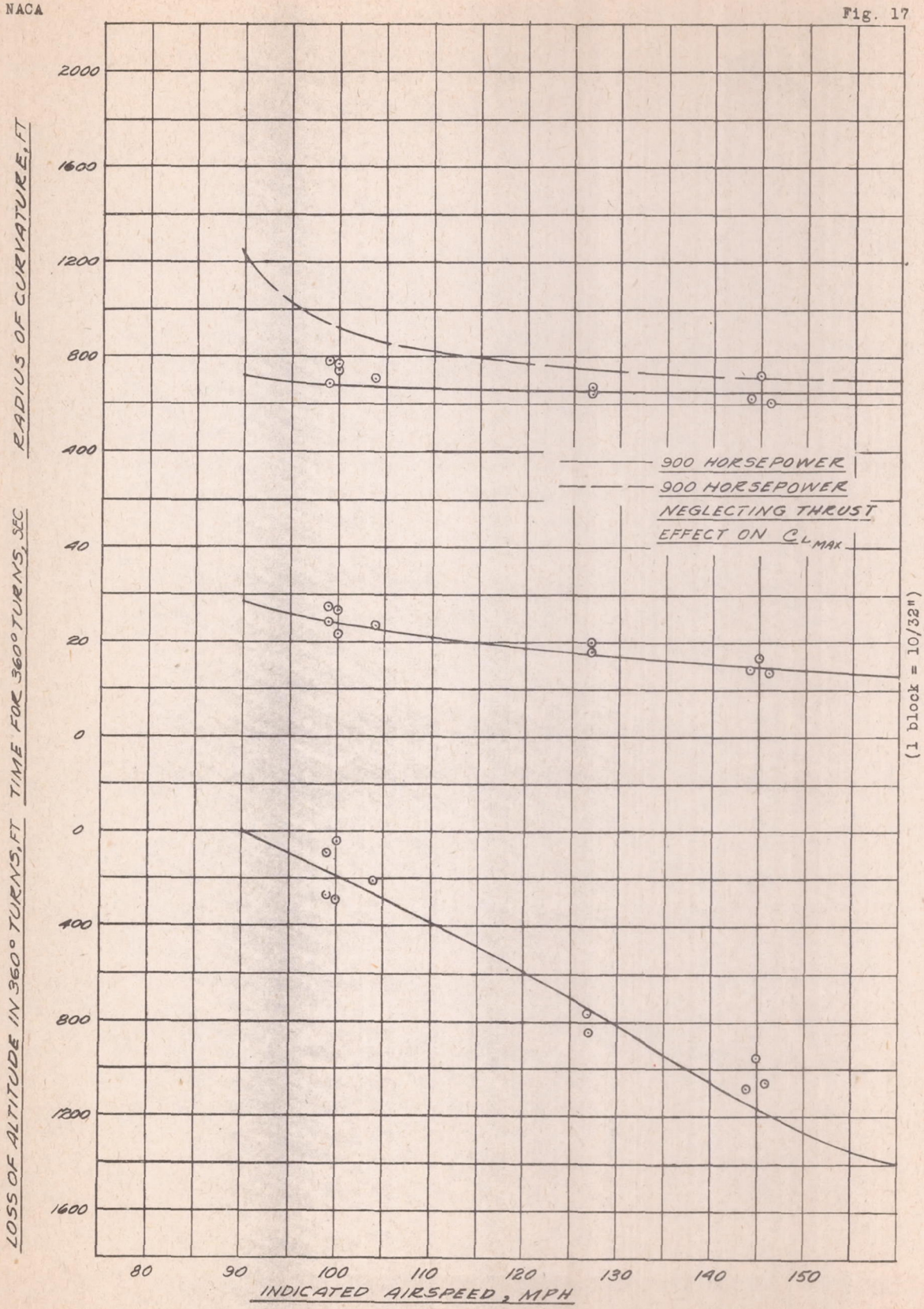

FIGURE 17- CALCULATED AND EXPERIMENTAL DETERMINATIONS OF THE TURNING PERFORMANCE, IN STEADY TURNS, AT 13000 FEET ALTITUDE, MAXIMUM LIFT COEFFICIENT, FLAPS 22° DOWN, NAVY F2A-3 AIRPLANE.

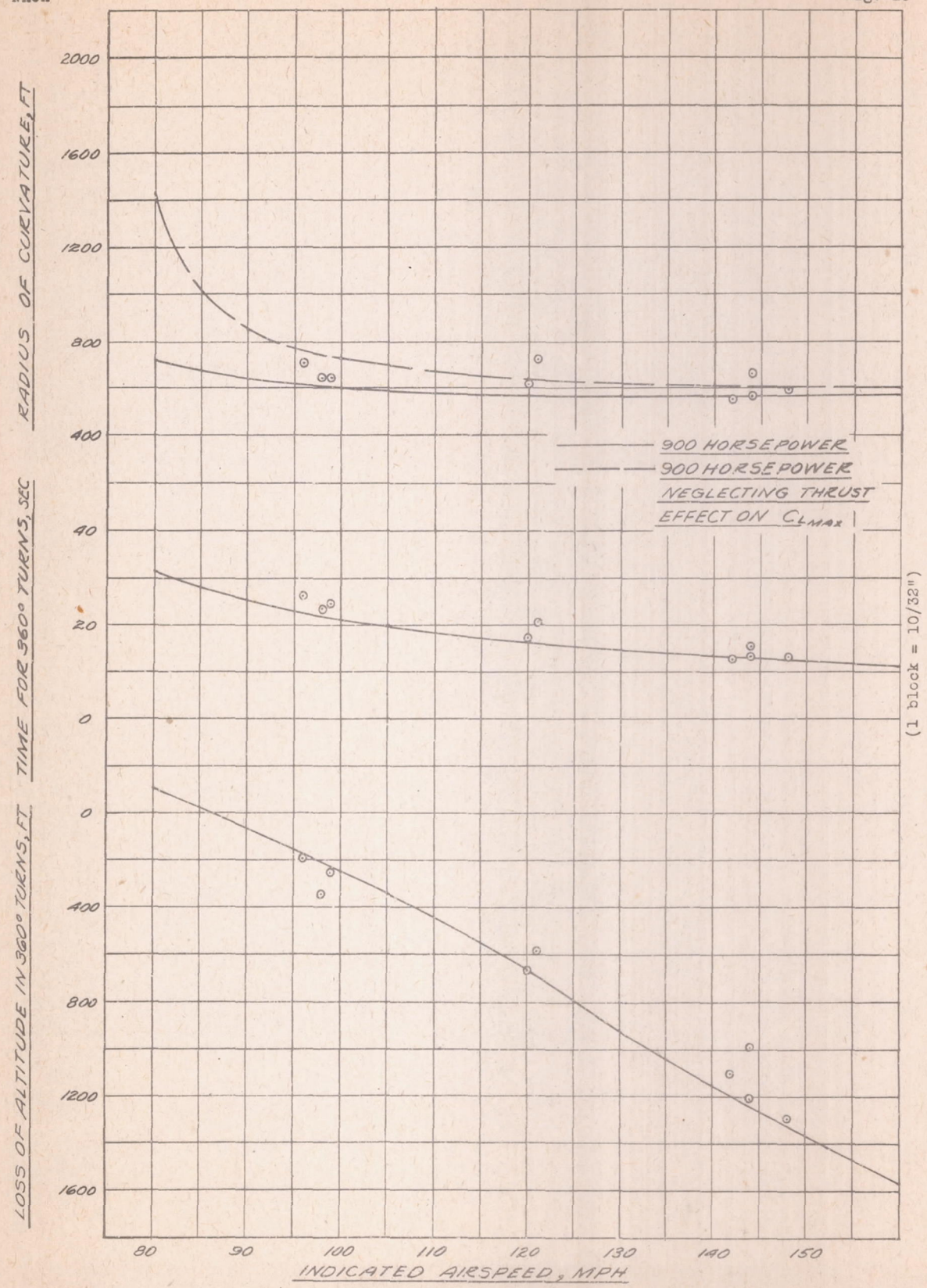

FIGURE 18.- CALCULATED AND EXPERIMENTAL DETERMINATIONS OF THE TURNING PERFORMANCE, IN STEADY TURNS, AT 13000 FEET ALTITUDE, MAXIMUM LIFT COEFFICIENT, FLAPS 56° DOWN OF A NAVY F2A-3 AIRPLANE.

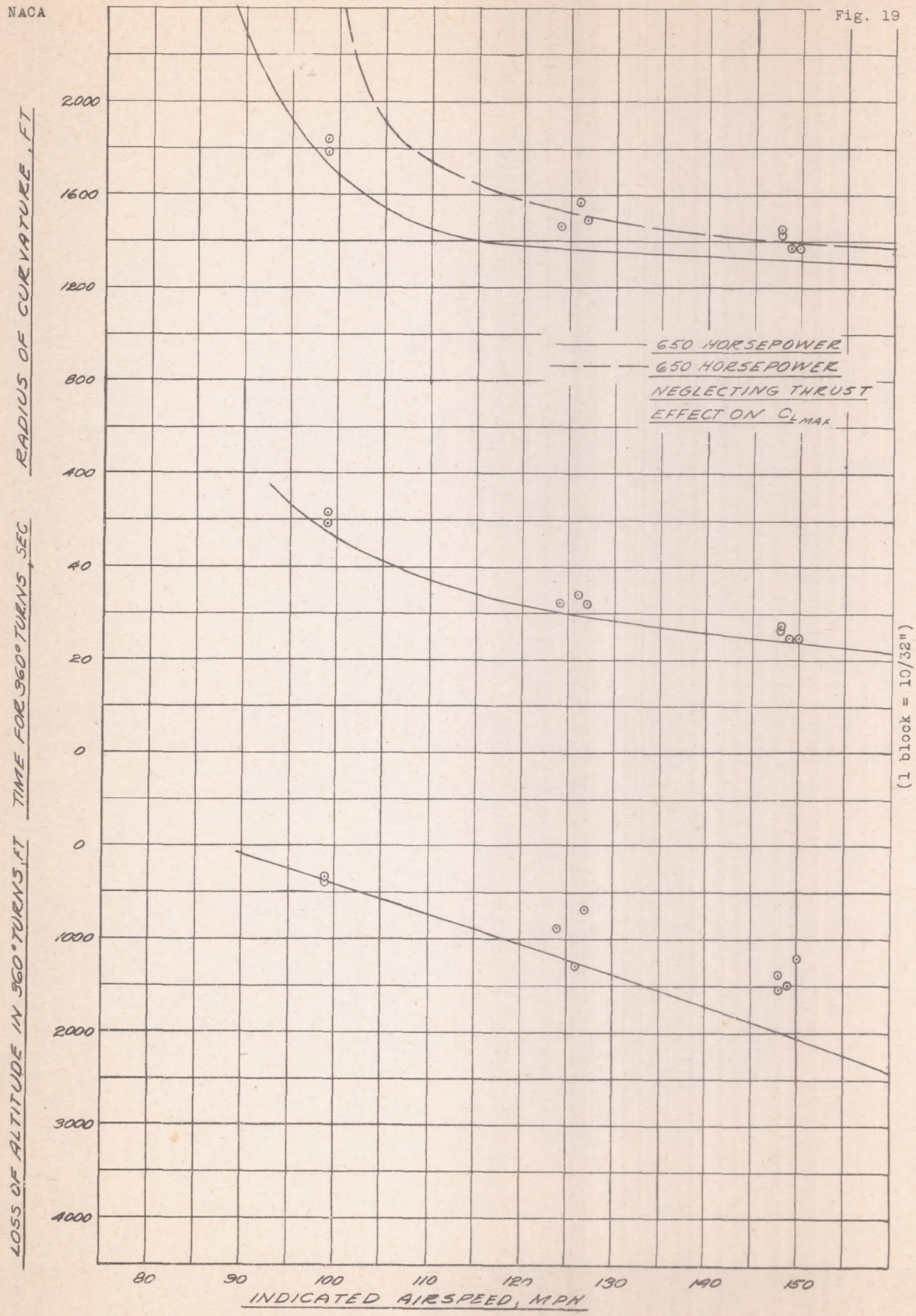

FIGURE 19.- CALCULATED AND EXPERIMENTAL DETERMINATIONS OF THE TURNING PERFORMANCE, IN STEADY TURNS, AT 27000 FEET ALTITUDE, MAXIMUM LIFT COEFFICIENT, FLAPS UP, OF A NAVY F2A-3 AIRPLANE.

NACA

Fig. 20

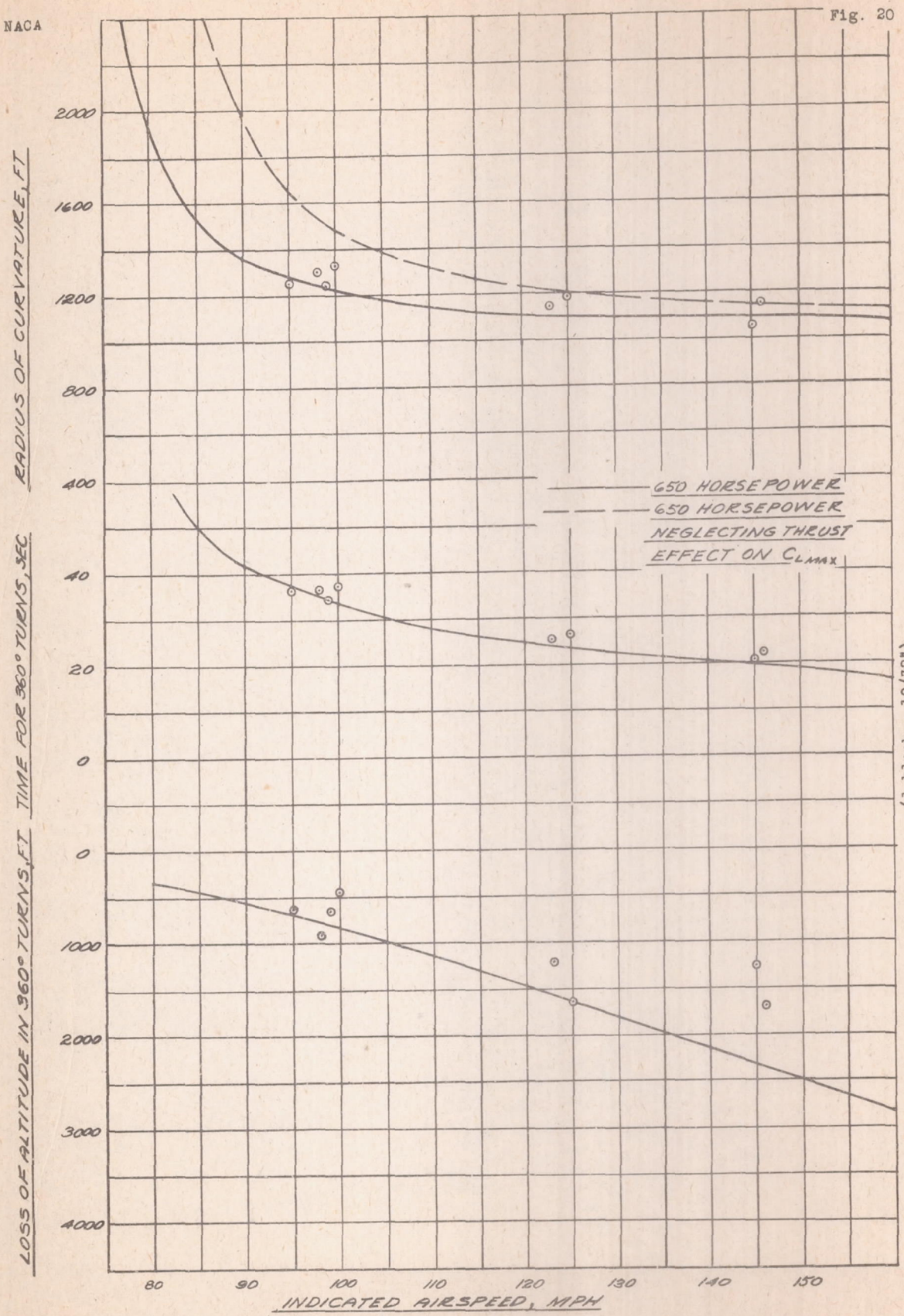

FIGURE 20.- CALCULATED AND EXPERIMENTAL DETERMINATIONS OF THE TURNING PERFORMANCE, IN STEADY TURNS, AT 27000 FEET ALTITUDE, MAXIMUM LIFT COEFFICIENT, FLAPS 22° DOWN OF A NAVY F2A-3 AIRPLANE.

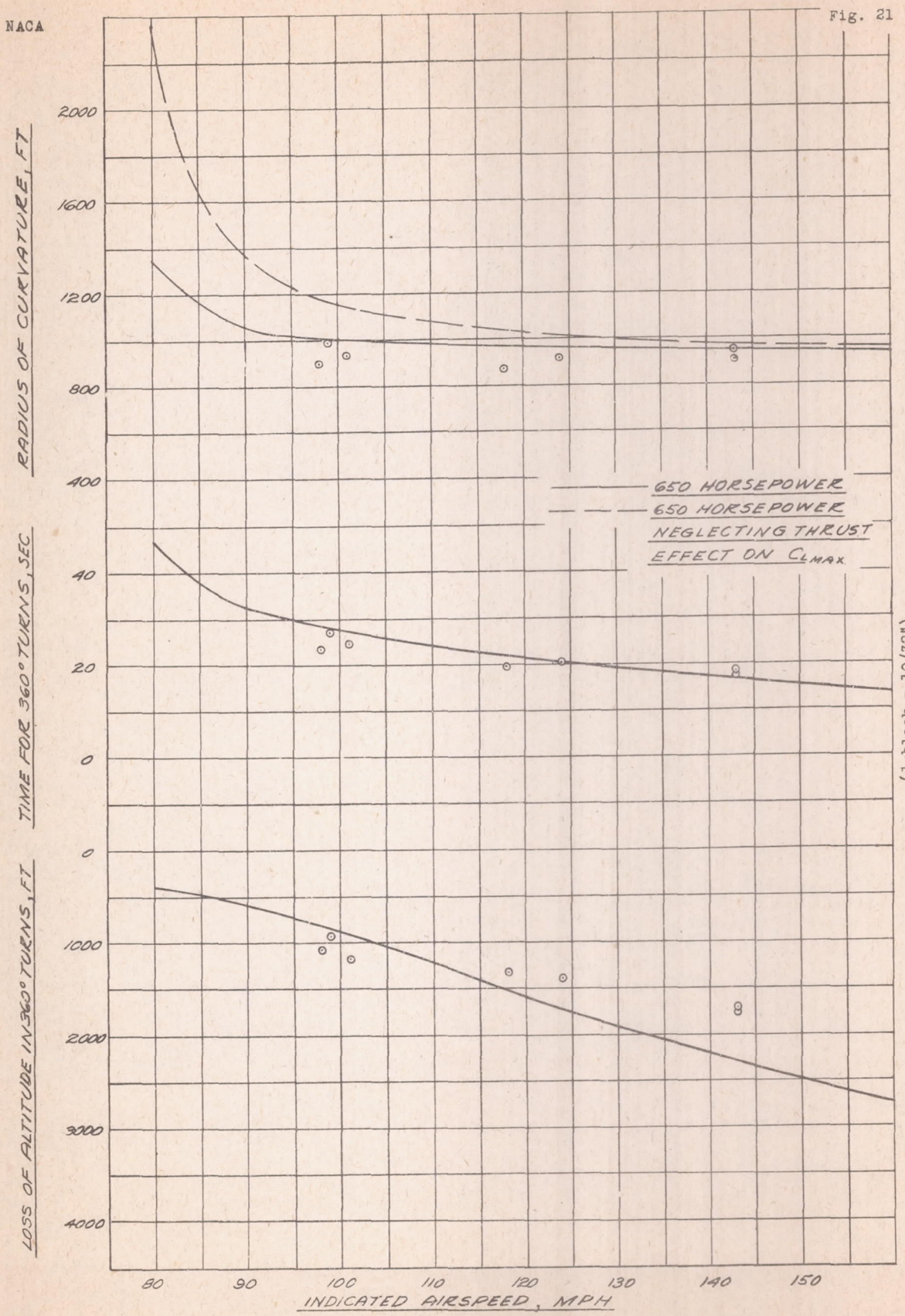

FIGURE 21.- CALCULATED AND EXPERIMENTAL DETERMINATIONS OF THE TURNING PERFORMANCE, IN STEADY TURNS, AT 27000 FEET ALTITUDE, MAXIMUM LIFT COEFFICIENT, FLAPS 56° DOWN, OF A NAVY F2A-3 AIRPLANE.

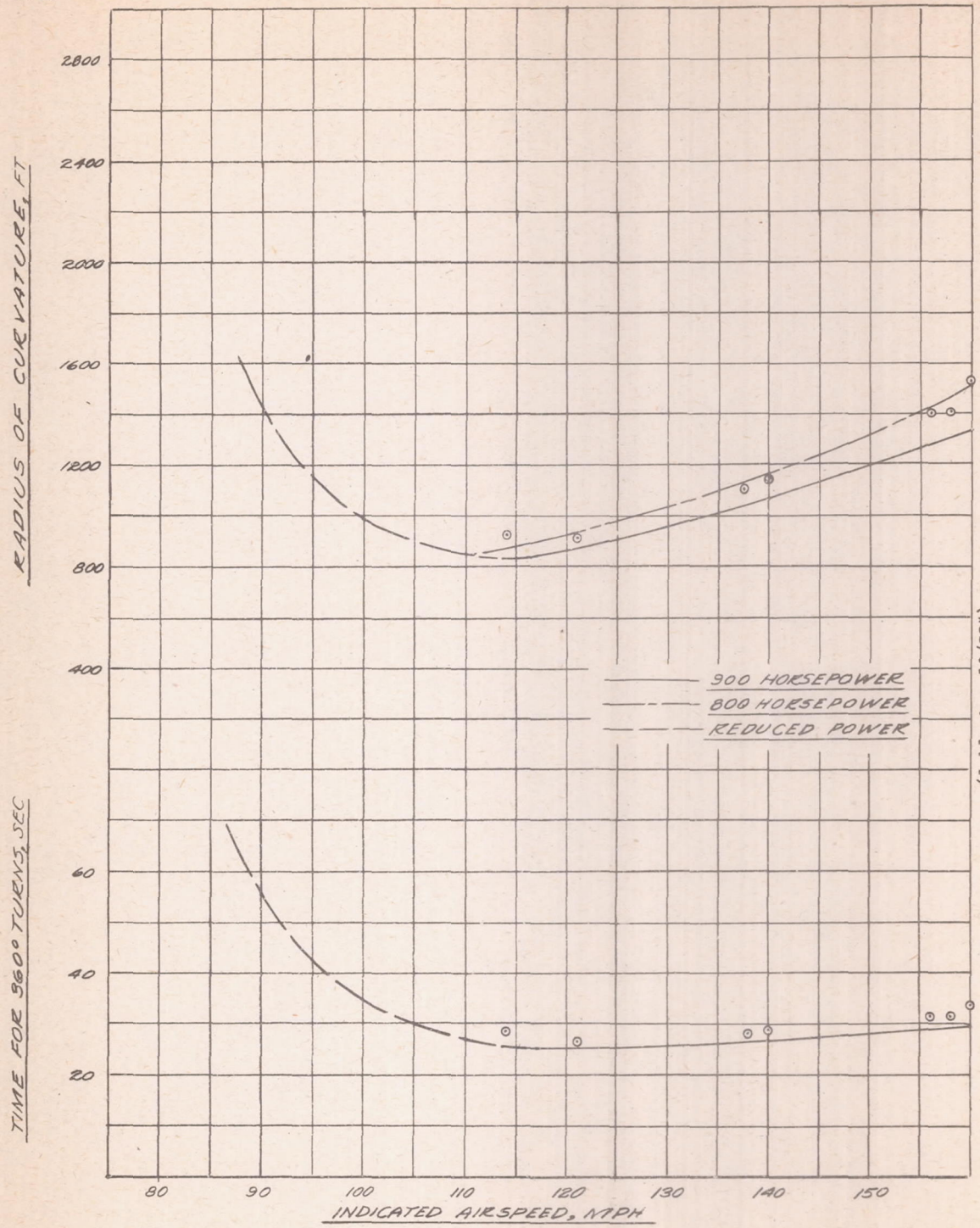

FIGURE 22.- CALCULATED AND EXPERIMENTAL DETERMINATIONS OF THE TURNING PERFORMANCE, IN STEADY HORIZONTAL TURNS, AT 13000 FEET ALTITUDE, FLAPS UP, OF A NAVY FRA-3 AIRPLANE.

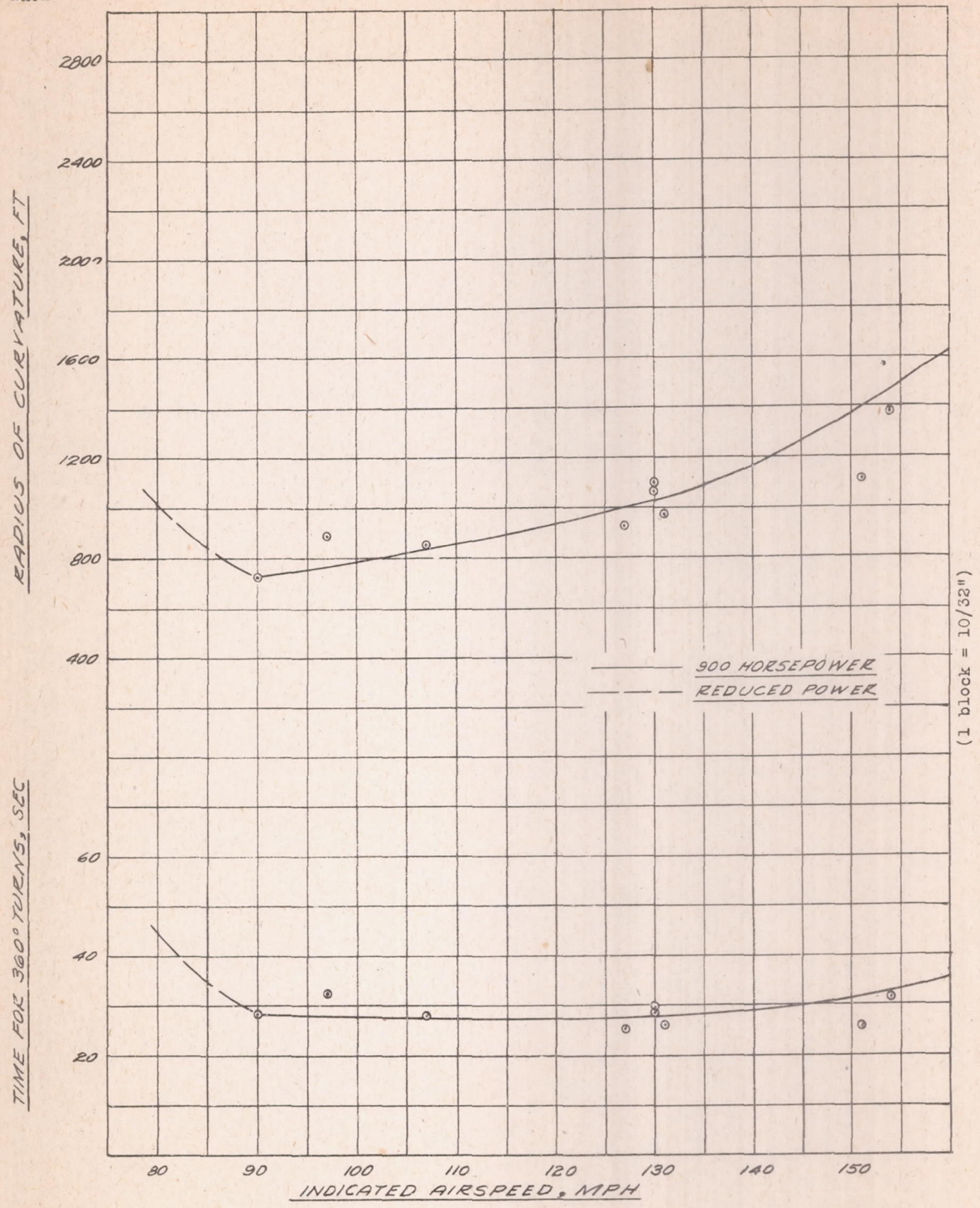

FIGUE 23.- CALCULATED AND EXPERIMENTAL DETERMINATIONS OF THE TURNING PERFORMANCE, IN STEADY HORIZONTAL TURNS, AT 13000 FEET ALTITUDE, FLAPS 22° DOWN, OF A NAVY F2A-3 AIRPLANE.

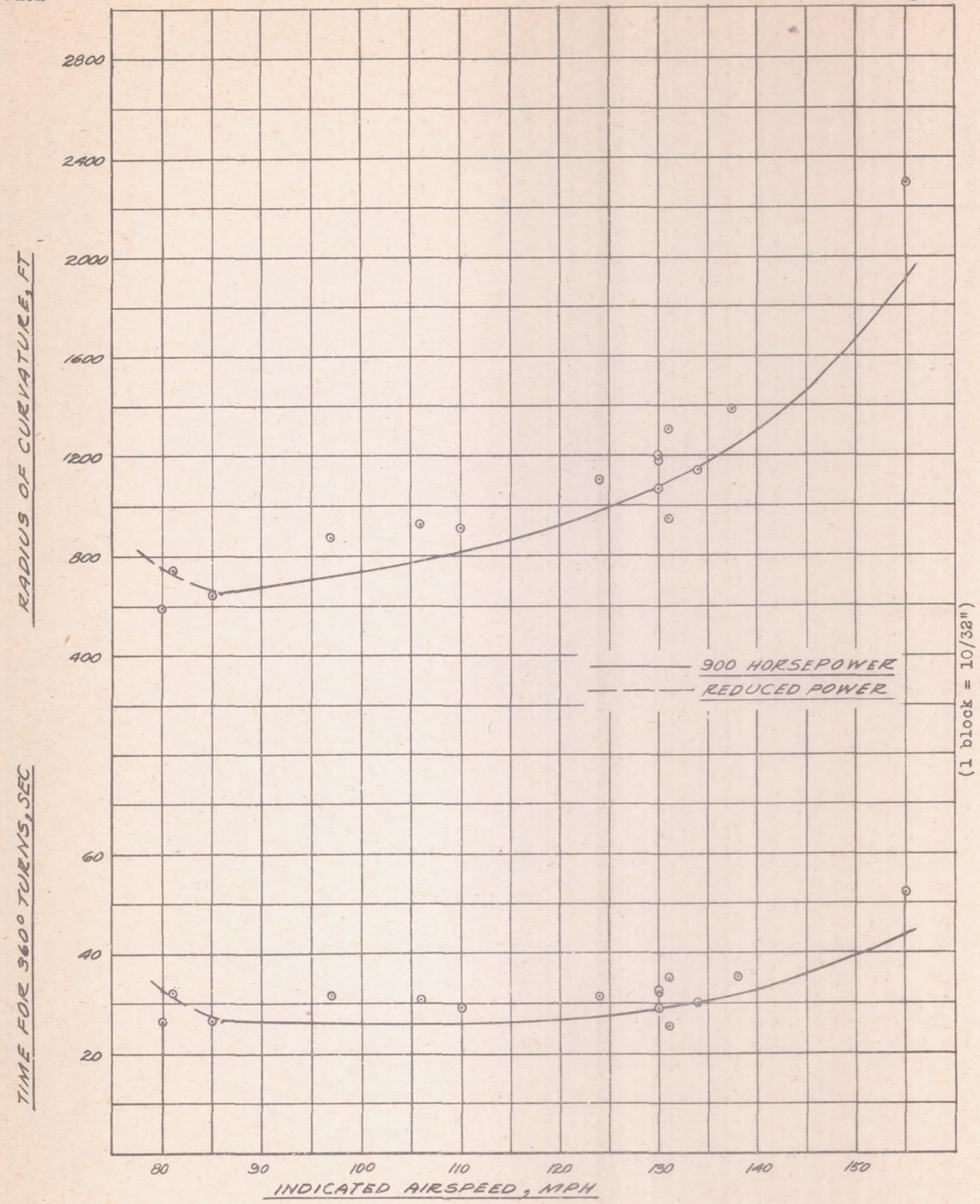

FIGURE 24.- CALCULATED AND EXPERIMENTAL DETERMINATIONS OF THE TURNING PERFORMANCE, IN STEADY HORIZONTAL TURNS, AT 13000 FEET ALTITUDE, FLAPS 56° DOWN, OF A NAVY F2A-3 AIRPLANE.

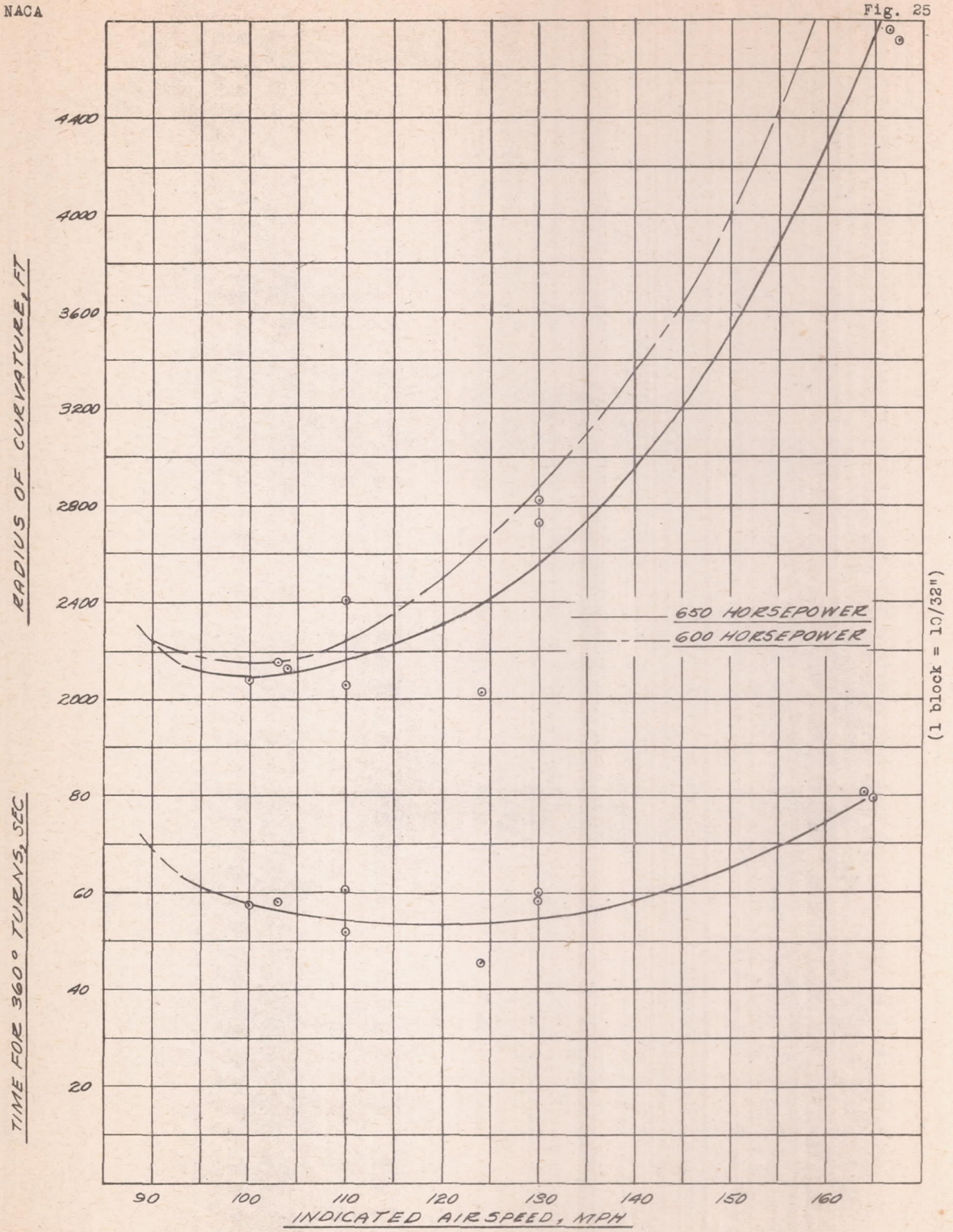

FIGURE 25.- CALCULATED AND EXPERIMENTAL DETERMINATIONS OF THE TURNING PERFORMANCE, IN STEADY HORIZONTAL TURNS, AT 27000 FEET ALTITUDE, FLAPS UP, OF A NAVY F2A-3 AIRPLANE.

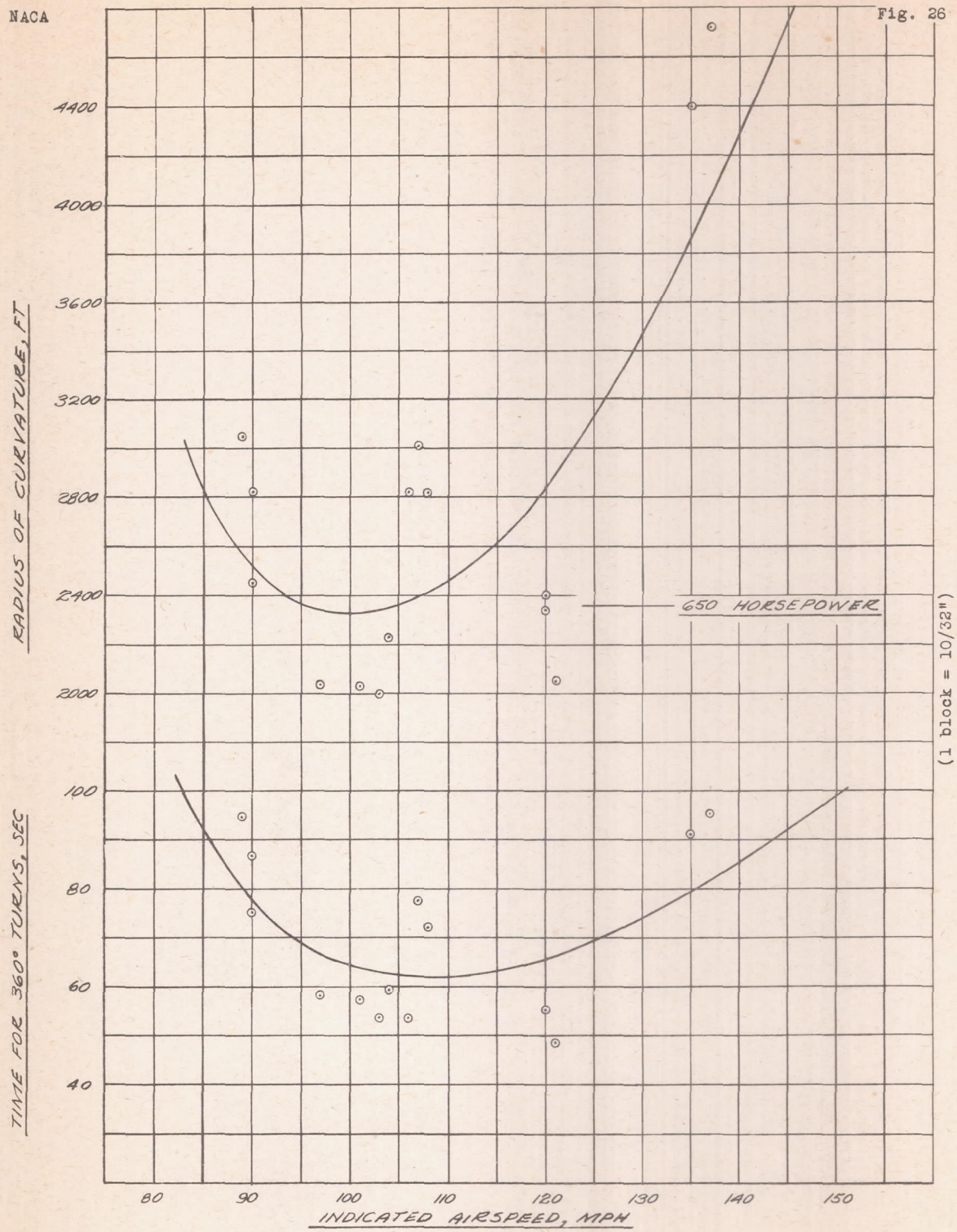

FIGURE 26.- CALCULATED AND EXPERIMENTAL DETERMINATIONS OF THE TURNING PERFORMANCE, IN STEADY HORIZONTAL TURNS, AT 27000 FEET ALTITUDE, FLAPS 22° DOWN, NAVY F2A-3 AIRPLANE.

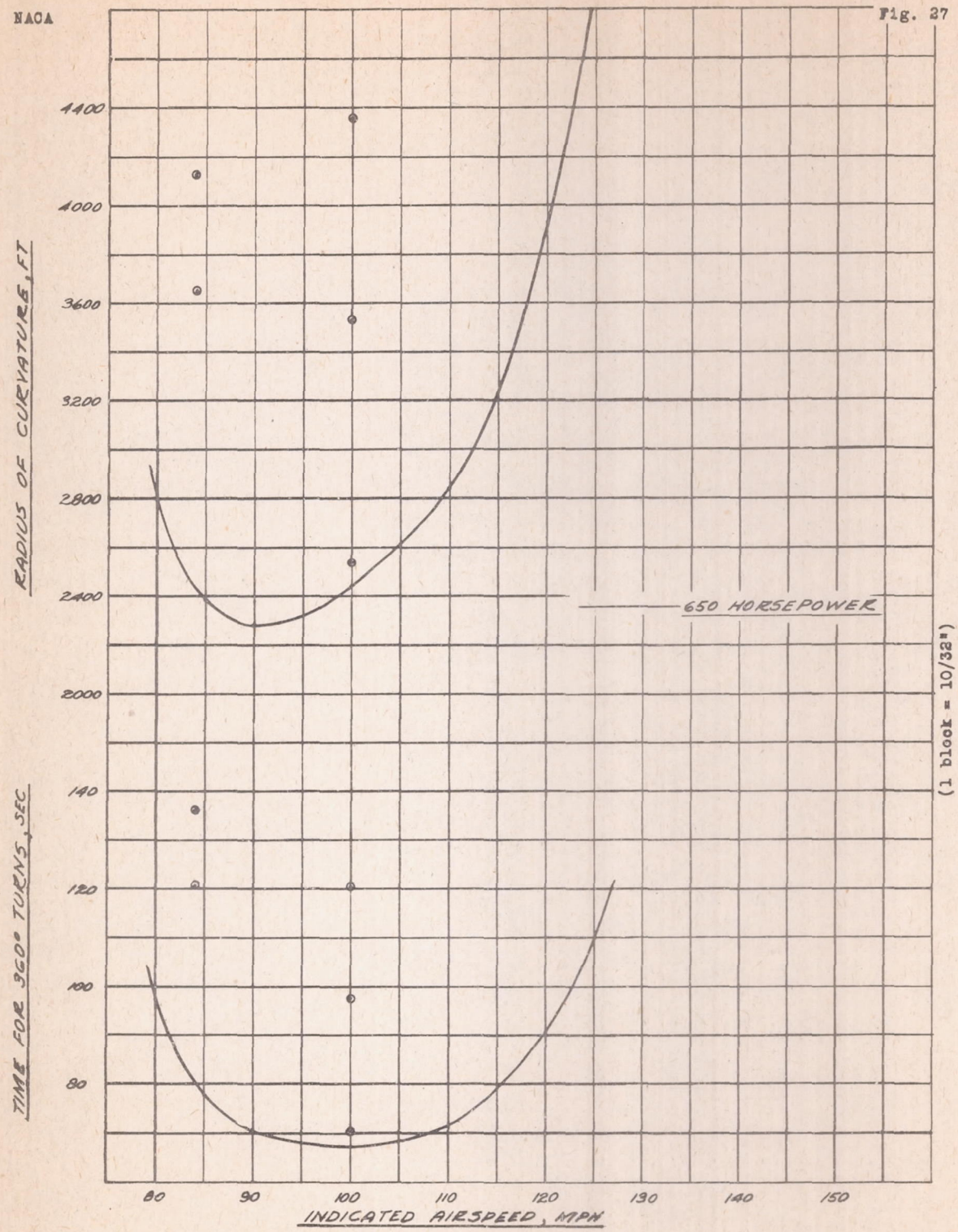

FIGURE 27.- CALCULATED AND EXPERIMENTAL DETERMINATIONS OF THE TURNING PERFORMANCE, IN STEADY HORIZONTAL TURNS, AT 27000 FEET ALTITUDE, FLAPS 56° DOWN, OF A NAVY F2A-3 AIRPLANE.

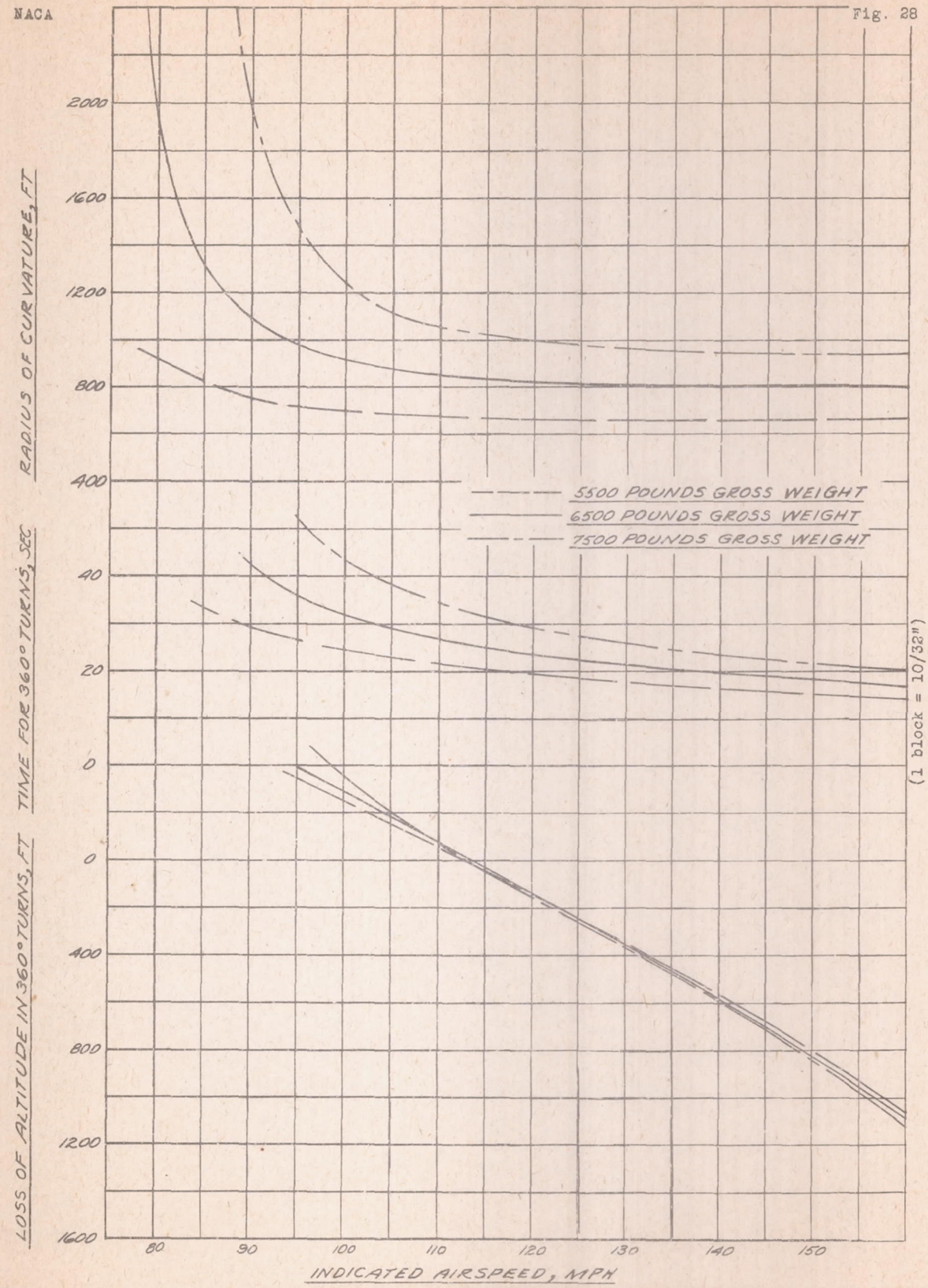

FIGURE 28.- VARIATIONS OF TURNING PERFORMANCE, DUE TO CHANGES OF WEIGHT, IN STEADY TURNS AT 13000 FEET ALTITUDE, MAXIMUM LIFT COEFFICIENT, FLAPS UP, 900 BRAKE HORSE-POWER, OF A NAVY F2A-3 AIRPLANE.

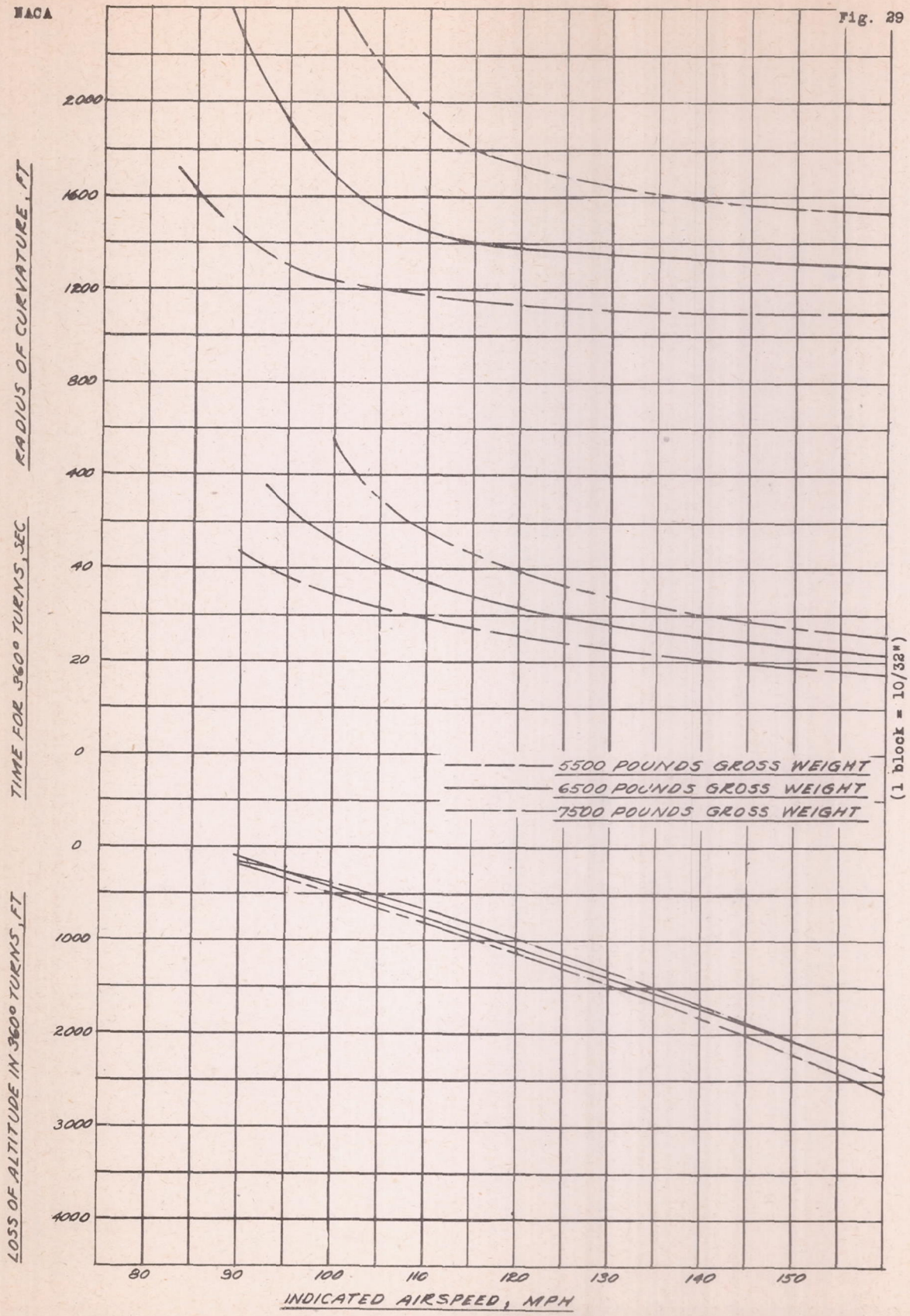

FIGURE 29.- VARIATIONS OF TURNING PERFORMANCE, DUE TO CHANGES OF WEIGHT, IN STEADY TURNS, AT 27000 FEET ALTITUDE, MAXIMUM LIFT COEFFICIENT, FLAPS UP, 650 BRAKE HORSEPOWER, OF A NAVY F2A-3 AIRPLANE.

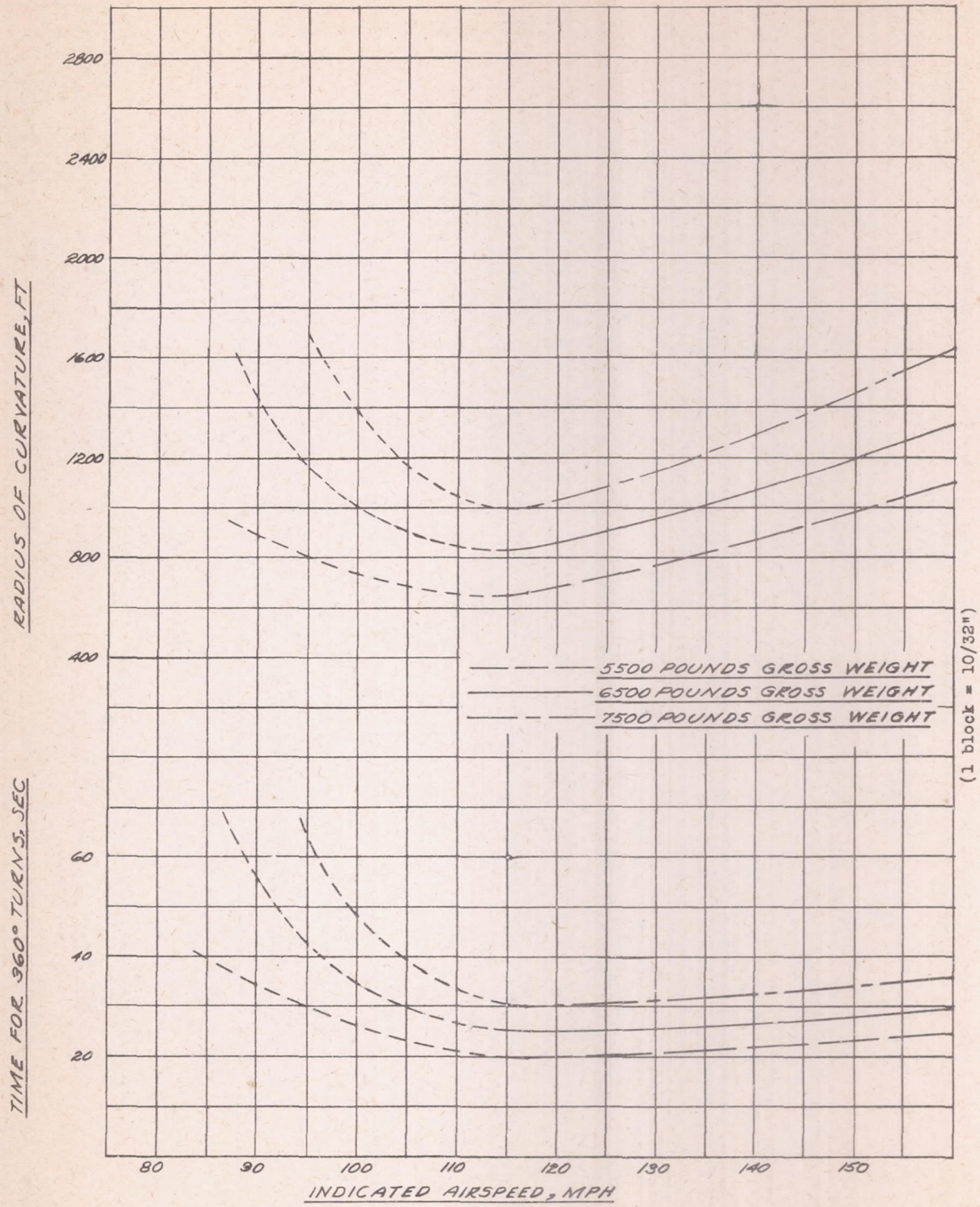

FIGURE 30.- VARIATIONS OF TURNING PERFORMANCE, DUE TO CHANGES OF WEIGHT, IN STEADY HORIZONTAL TURNS, AT 13000 FEET ALTITUDE, FLAPS UP, 900 BRAKE HORSEPOWER, OF A NAVY F2A-3 AIRPLANE.

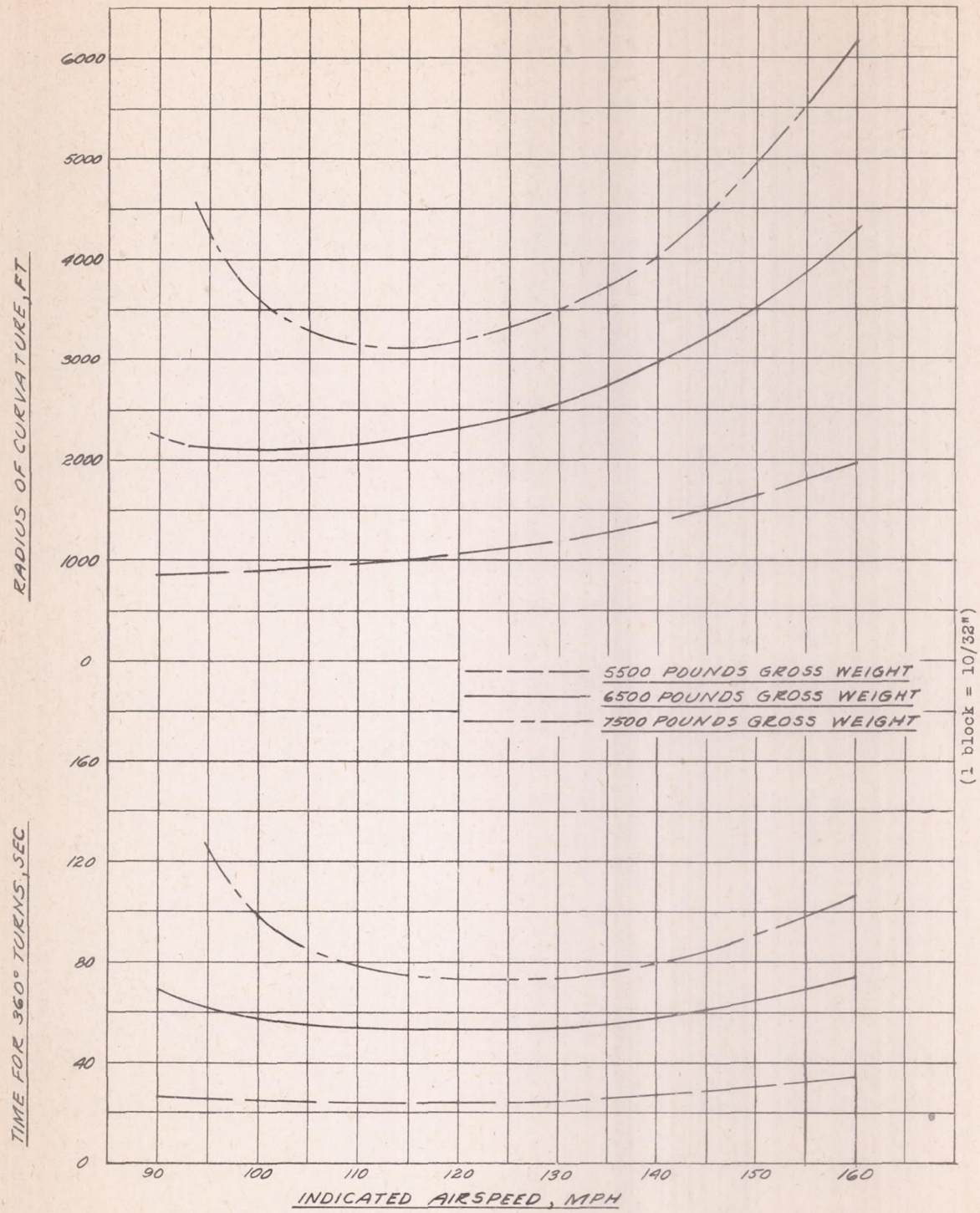

FIGURE 31 - VARIATIONS OF TURNING PERFORMANCE, DUE TO CHANGES OF WEIGHT, IN STEADY HORIZONTAL TURNS, AT 27000 FEET ALTITUDE, FLAPS UP, 650 BRAKE HORSEPOWER, OF A NAVY F2A-3 AIRPLANE.

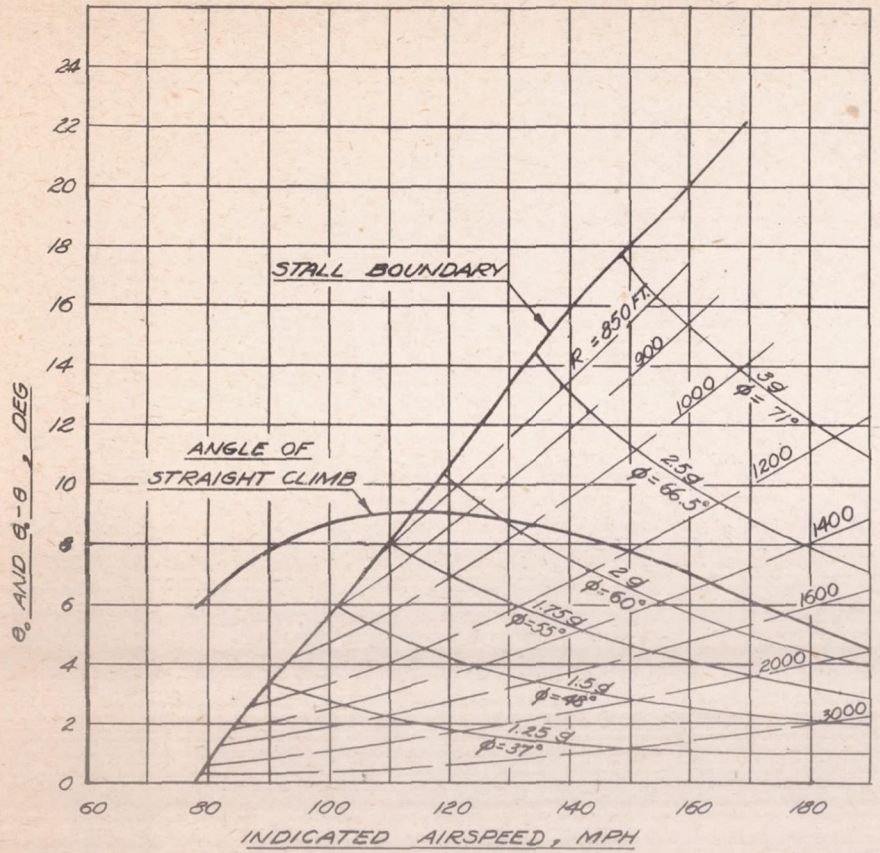

(1 block = 10/32")

FIGURE 32.- TURNING PERFORMANCE DIAGRAM, 13000 FEET ALTITUDE, 900 BRAKEHORSEPOWER, FLAPS UP, NAVY F2A-3 AIRPLANE.

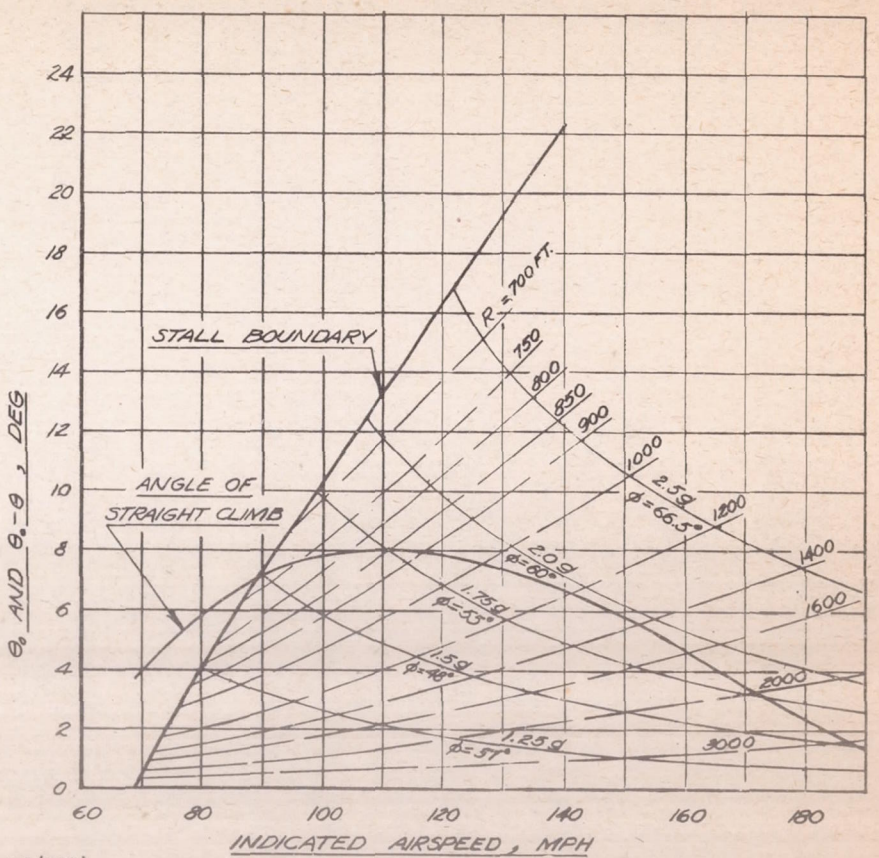

FIGURE 33.- TURNING PERFORMANCE DIAGRAM, 13000 FEET ALTITUDE, 900 BRAKE HORSEPOWER, FLAPS 22° DOWN, NAVY F2A-3 AIRPLANE.

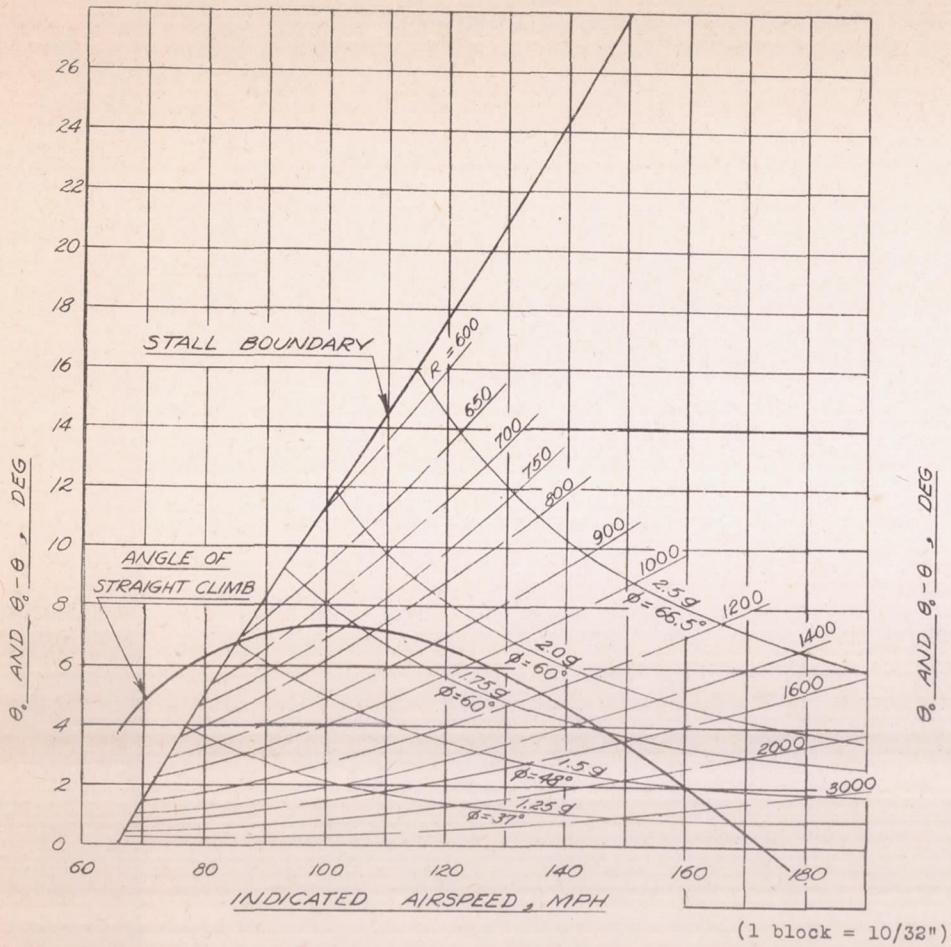

FIGURE 34.- TURNING PERFORMANCE DIAGRAM, 13000 FEET ALTITUDE, 900 BRAKE HORSEPOWER, FLAPS 56° DOWN, NAVY F2A-3 AIRPLANE.

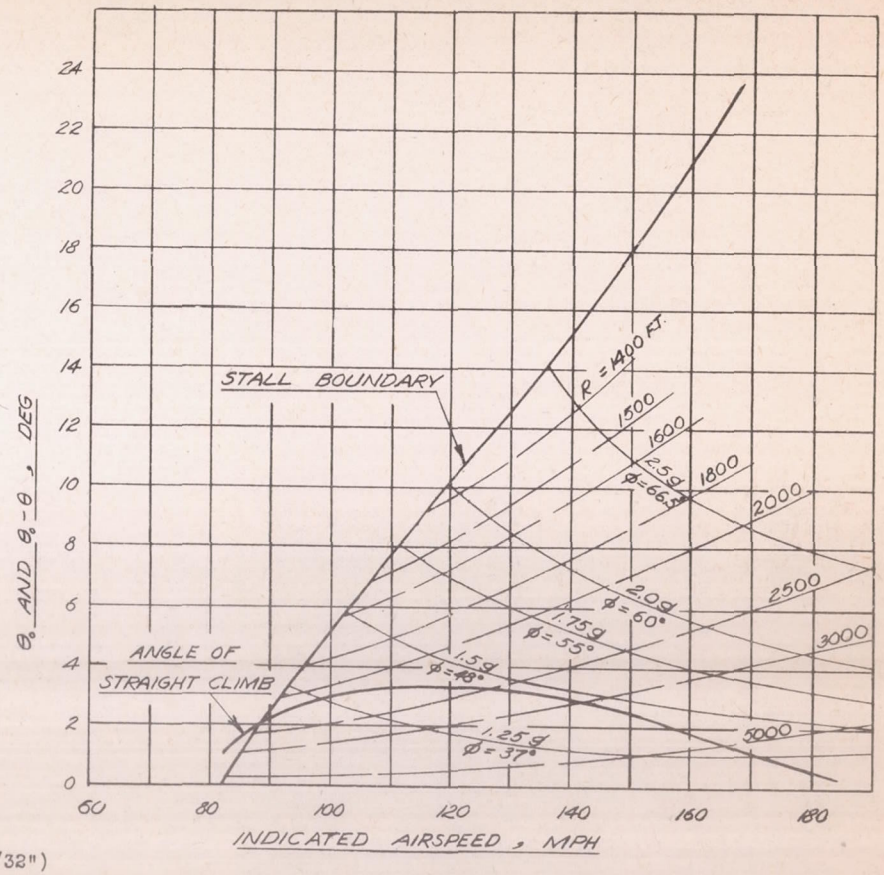

FIGURE 35.- TURNING PERFORMANCE DIAGRAM, 27000 FEET ALTITUDE, 650 BRAKE HORSEPOWER, FLAPS UP, NAVY F2A-3 AIRPLANE.

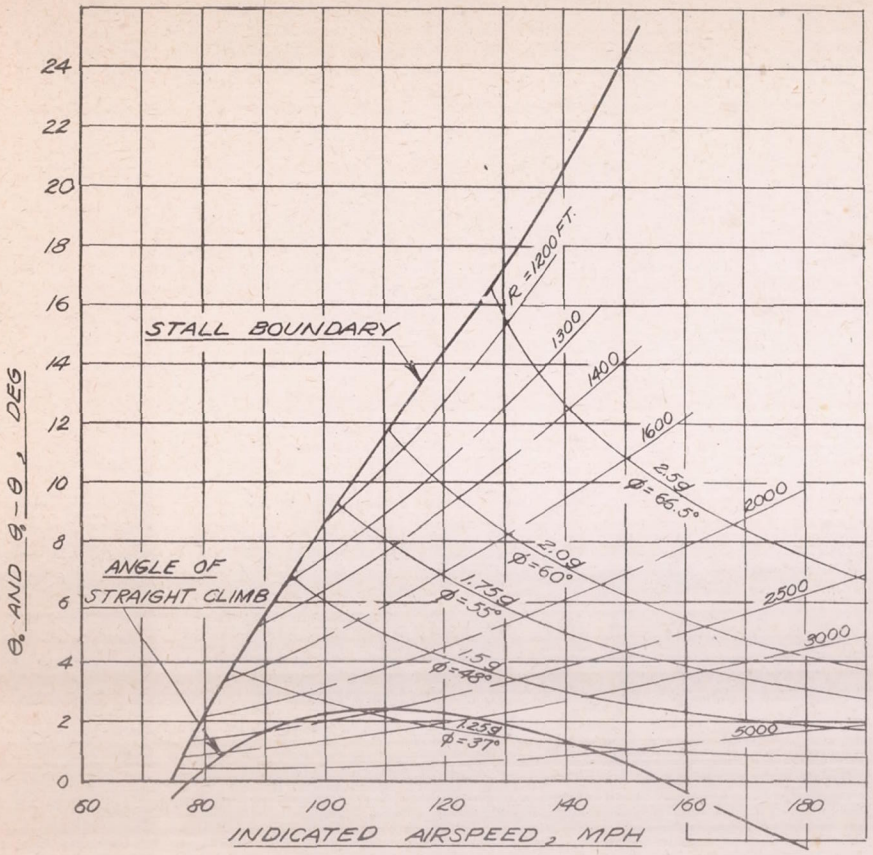

FIGURE 36.- TURNING PERFORMANCE DIAGRAM, 27000 FEET ALTITUDE, 650 BRAKE HORSEPOWER FLAPS 22° DOWN, NAVY F2A-3 AIRPLANE

(1 block = 10/32")

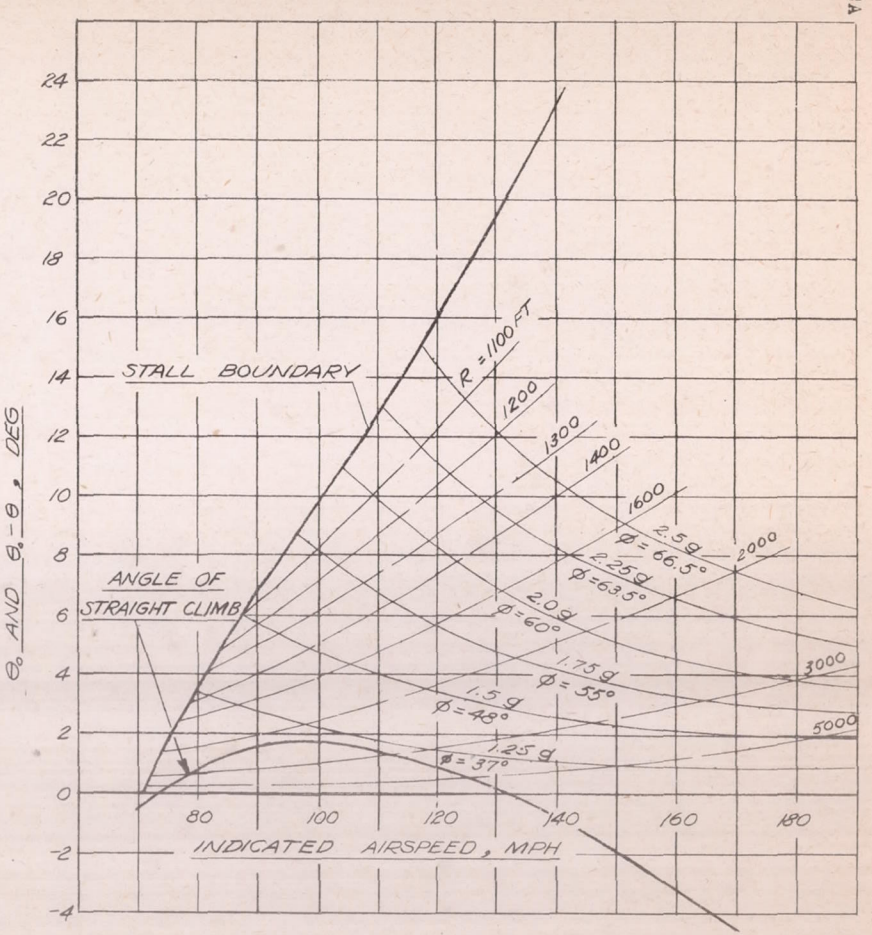

FIGURE 37.- TURNING PERFORMANCE DIAGRAM, 27000 FEET ALTITUDE, 650 BRAKE HORSEPOWER, FLAPS 56° DOWN, NAVY F2A-3 AIRPLANE.

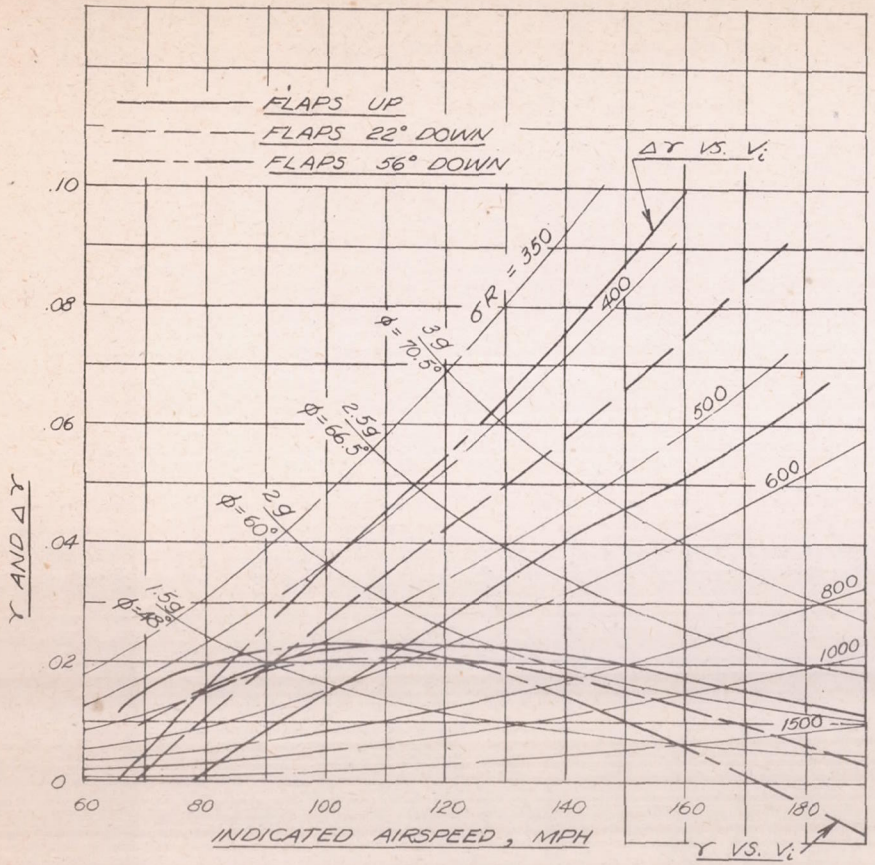

(1 block = 10/32")

FIGURE 38:- TURNING PERFORMANCE DIAGRAM, 13000 FEET ALTITUDE, 900 BRAKE HORSEPOWER, NAVY F2A-3 AIRPLANE.

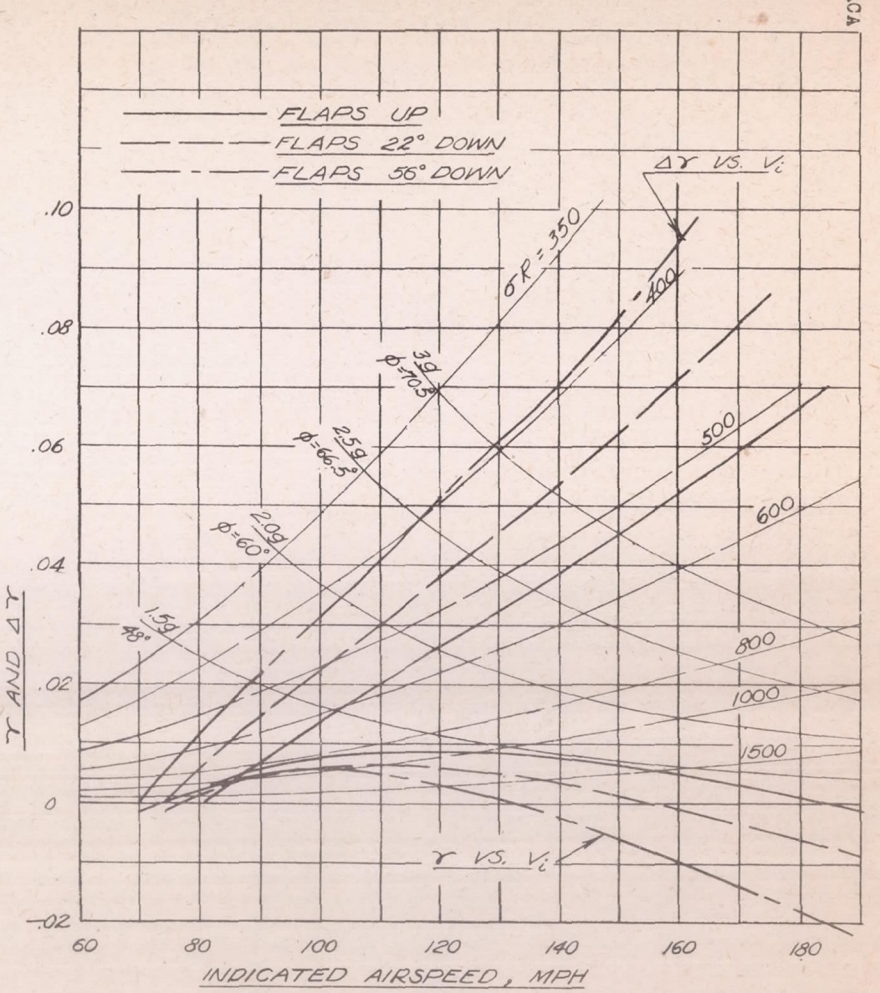

FIGURE 39:- TURNING PERFORMANCE DIAGRAM, 27000 FEET ALTITUDE, 650 BRAKE HORSEPOWER, NAVY F2A-3 AIRPLANE.